

AD695619

MISCELLANEOUS PAPER NO. 4-980

FACTORS THAT INFLUENCE THE DEVELOPMENT OF SOIL CONSTITUTIVE RELATIONS

by

J. G. Jackson, Jr.



July 1968

Sponsored by

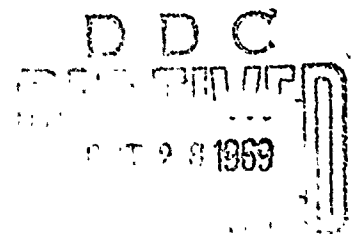
Defense Atomic Support Agency

Conducted by

U. S. Army Engineer Waterways Experiment Station
CORPS OF ENGINEERS
Vicksburg, Mississippi

THIS DOCUMENT HAS BEEN APPROVED FOR PUBLIC RELEASE
AND SALE; ITS DISTRIBUTION IS UNLIMITED

U.S. GOVERNMENT
CLEARINGHOUSE
1601 Center for the Study of the History of the
United States Government, Washington, D.C. 20540



41

DISCLAIMER NOTICE

**THIS DOCUMENT IS BEST QUALITY
PRACTICABLE. THE COPY FURNISHED
TO DTIC CONTAINED A SIGNIFICANT
NUMBER OF PAGES WHICH DO NOT
REPRODUCE LEGIBLY.**

ACCESSION FOR	
CFSTI	WHITE SECTION <input checked="" type="checkbox"/>
DDC	BUFF SECTION <input type="checkbox"/>
UNANNOUNCED	<input type="checkbox"/>
JUSTIFICATION	
V	
DISTRIBUTION/AVAILABILITY CODES	
DIST.	AVAIL. and/or SPECIAL
1	

Destroy this report when no longer needed. Do not return it to the originator.

The findings in this report are not to be construed as an official Department of the Army position, unless so designated by other authorized documents.

Typical Stress-Strain Response

An excellent example of the typical shape of a uniaxial stress-strain curve for in-situ soils is given by the results shown in Figure 1 for a static load-unload test conducted on undisturbed specimen No. HV 5.8.1 taken from the Minuteman HEST Test V site in North Dakota. The usual S-shape of the virgin loading curve results from an initial resistance due to natural cementation and geostatic overburden effects followed by a softening as these effects are overcome by the applied live-load stress; thereafter, the curve gradually stiffens as the soil densifies, becoming quite steep as the air voids are closed and the specimen saturates. This distinct nonlinear behavior means, of course, that wave propagation cannot be characterized by a single compression wave velocity but, theoretically, by an infinite number of incremental stress wave speeds.

The unloading curve is also nonlinear and is initially quite steep, indicating that rarefaction or unloading waves will generally travel much faster than compression waves. It also indicates that the material is quite inelastic, which results in a hysteretic strain energy loss or damping with each load cycle. This is due to the fact that soils are not "solid" but are in fact mixtures of air, water, and solid particles. The ability of a particular soil sample to "recover" compressive strain largely depends on the relative percentages of each of these three composites in the mixture.

Loading Rate Effects

Dynamic stress-strain curves are also characterized by nonlinear-inelastic behavior as indicated by the results shown in Figure 2 for test No. HV 5.8.3. This specimen came from the same HEST Test V Shelby-tube sample as the specimen for the static test, No. HV 5.8.1; classification and index test showed them to be almost identical. The influence of loading rate for this material is indicated on Figure 2 by the loading curve (dashed line) for the static test No. HV 5.8.1 (extracted from Figure 1). The implication is that, while considerable information regarding basic behavior patterns can be obtained from static tests, quantitative data for use in computer code calculations should be obtained from dynamic tests which apply impulsive loadings with magnitudes and time-histories similar to those expected in the field problems being calculated.

Unloading-Reloading Effects

The stress-history for the impulsive loading applied in test No. HV 5.8.3 (Figure 2) shows several significant unload-reload oscillations after the maximum stress has been reached. The effect of these oscillations on the stress-strain curve is also shown and indicates quite

FOREWORD

This paper presents results from research on propagation of ground shock through soils being conducted by personnel of the Soils Division, U. S. Army Engineer Waterways Experiment Station. The work is sponsored by the Defense Atomic Support Agency (DASA).

This paper was prepared for presentation at the DASA Long Range Planning Meeting in Strategic Structures Vulnerability/Hardening held at the Air Force Weapons Laboratory, Kirtland AFB, 30 January - 1 February 1968.

CONTENTS

	<u>Page</u>
FOREWORD.	iii
CONVERSION FACTORS, BRITISH TO METRIC UNITS OF MEASUREMENT.	vii
ABSTRACT.	ix
INTRODUCTION.	1
UNIAXIAL STRAIN TEST RESULTS.	2
Typical Stress-Strain Response.	3
Loading Rate Effects.	3
Unloading-Reloading Effects	3
Degree of Saturation Effects.	6
Unexpected Subsurface Layers.	6
Weathering Effects.	14
Geostatic Stress Effects.	14
Application of Data to Computer Codes	20
TRIAXIAL COMPRESSION TEST RESULTS	24
Shear Strength Data	24
Yield Criteria for Computer Codes	30
Stress-Strain Data.	32
CONCLUSION.	32
REFERENCES.	36

CONVERSION FACTORS, BRITISH TO METRIC UNITS OF MEASUREMENT

British units of measurement used in this report can be converted to metric units as follows:

<u>Multiply</u>	<u>By</u>	<u>To Obtain</u>
inches	25.4	millimeters
feet	30.48	centimeters
pounds per square inch	0.070307	kilograms per square centimeter
pounds per cubic foot	16.0185	kilograms per cubic meter
kips per square inch	70.307	kilograms per square centimeter

ABSTRACT

Computer codes which attempt to solve free-field ground shock problems should be based on mathematically defined constitutive models which realistically simulate the behavior of actual earth materials. Laboratory uniaxial strain and triaxial compression test data are presented to illustrate the effects of various factors such as loading rate, history of unloading-reloading, degree of saturation, weathering, geostatic stress and confining pressure on the stress-strain and strength properties used in soil constitutive relations.

The factor which stands out as having by far the most influence on constitutive behavior is the state of stress to which the soil sample (or earth mass) is subjected. An attempt is being made to develop a completely nonlinear-inelastic constitutive model that, when subjected to the particular state of stress used in a laboratory property test, will essentially mirror the test results.

J. G. Jackson, Jr.
U. S. Army Engineer Waterways Experiment Station

FACTORS THAT INFLUENCE THE DEVELOPMENT OF SOIL CONSTITUTIVE RELATIONS

INTRODUCTION

Free-field ground shock problems involve extremely difficult geometries and boundary loading conditions to the extent that the only hope for obtaining quantitative solutions (or "numbers") is through numerical approximation schemes or computer codes. Such simulation may involve a succession of several codes, i.e., a radiation transport code followed by a close-in cratering and hydrodynamic code followed by a solid mechanics code for treating compressible, shear-resisting materials.

It is the solid-model codes that are of primary interest in the work being done by WES under DASA Subtask RSS2209, "Propagation of Ground Shock Through Soils." The intent of this paper is to present a general discussion of various factors which influence the development of soil constitutive relations for the "solid" regime. In order to make it as practical and as up-to-date as possible, these factors will be illustrated with specific examples of actual test data developed in support of several current calculation projects.

All of the currently programmed mathematical relations used to define stress-strain behavior within simulated earth "solids" are rooted from the classical linear elastic constitutive relation

$$\sigma_{ij} = \lambda e \delta_{ij} + 2\mu \epsilon_{ij}$$

where

σ_{ij} = total stress tensor

ϵ_{ij} = total strain tensor

δ_{ij} = Kronecker delta function

$$e = \epsilon_{kk} = \epsilon_{11} + \epsilon_{22} + \epsilon_{33}$$

λ & μ = Lamé constants

For code applications, this tensor relation is usually rewritten in terms of pure compression and pure shear components, i.e.,

$$\sigma_{ij} = K e \delta_{ij} + 2G \epsilon'_{ij}$$

where

$$\sigma_{ij} = p\delta_{ij} + \sigma'_{ij}$$

$$p = 1/3 \sigma_{kk} = 1/3 (\sigma_{11} + \sigma_{22} + \sigma_{33})$$

$$\epsilon'_{ij} = \epsilon_{ij} - 1/3 \epsilon \delta_{ij}$$

$$K = \text{bulk modulus} = \frac{p}{\epsilon}$$

$$G = \text{shear modulus} = \frac{1}{2} \frac{\sigma'_{ij}}{\epsilon'_{ij}}$$

Since our problems are dynamic, we are concerned with the influence of constitutive properties on the propagation of waves. In an infinite elastic medium

$$v_p = \sqrt{\frac{\lambda + 2\mu}{\rho}} = \sqrt{\frac{K + 4G/3}{\rho}} = \sqrt{\frac{M}{\rho}}$$

and $v_s = \sqrt{\frac{G}{\rho}}$

where

v_p = compression wave velocity

v_s = shear wave velocity

ρ = mass density

M = constrained modulus

This linking between compression wave velocity and constrained modulus has probably been the major influence motivating most of the blast-oriented soil property testing since 1960.

UNIAXIAL STRAIN TEST RESULTS

Constrained modulus is determined in the laboratory by axially compressing cylindrical soil samples in a uniaxial strain device (one-dimensional compression device or oedometer)¹ and measuring their axial strain response; i.e., the slope of the relation between axial stress and axial strain, under conditions of zero radial strain, defines the constrained modulus.

Typical Stress-Strain Response

An excellent example of the typical shape of a uniaxial stress-strain curve for in-situ soils is given by the results shown in Figure 1 for a static load-unload test conducted on undisturbed specimen No. HV 5.8.1 taken from the Minuteman HEST Test V site in North Dakota. The usual S-shape of the virgin loading curve results from an initial resistance due to natural cementation and geostatic overburden effects followed by a softening as these effects are overcome by the applied live-load stress; thereafter, the curve gradually stiffens as the soil densifies, becoming quite steep as the air voids are closed and the specimen saturates. This distinct nonlinear behavior means, of course, that wave propagation cannot be characterized by a single compression wave velocity but, theoretically, by an infinite number of incremental stress wave speeds.

The unloading curve is also nonlinear and is initially quite steep, indicating that rarefaction or unloading waves will generally travel much faster than compression waves. It also indicates that the material is quite inelastic, which results in a hysteretic strain energy loss or damping with each load cycle. This is due to the fact that soils are not "solid" but are in fact mixtures of air, water, and solid particles. The ability of a particular soil sample to "recover" compressive strain largely depends on the relative percentages of each of these three composites in the mixture.

Loading Rate Effects

Dynamic stress-strain curves are also characterized by nonlinear-inelastic behavior as indicated by the results shown in Figure 2 for test No. HV 5.8.3. This specimen came from the same HEST Test V Shelby-tube sample as the specimen for the static test, No. HV 5.8.1; classification and index test showed them to be almost identical. The influence of loading rate for this material is indicated on Figure 2 by the loading curve (dashed line) for the static test No. HV 5.8.1 (extracted from Figure 1). The implication is that, while considerable information regarding basic behavior patterns can be obtained from static tests, quantitative data for use in computer code calculations should be obtained from dynamic tests which apply impulsive loadings with magnitudes and time-histories similar to those expected in the field problems being calculated.

Unloading-Reloading Effects

The stress-history for the impulsive loading applied in test No. HV 5.8.3 (Figure 2) shows several significant unload-reload oscillations after the maximum stress has been reached. The effect of these oscillations on the stress-strain curve is also shown and indicates quite

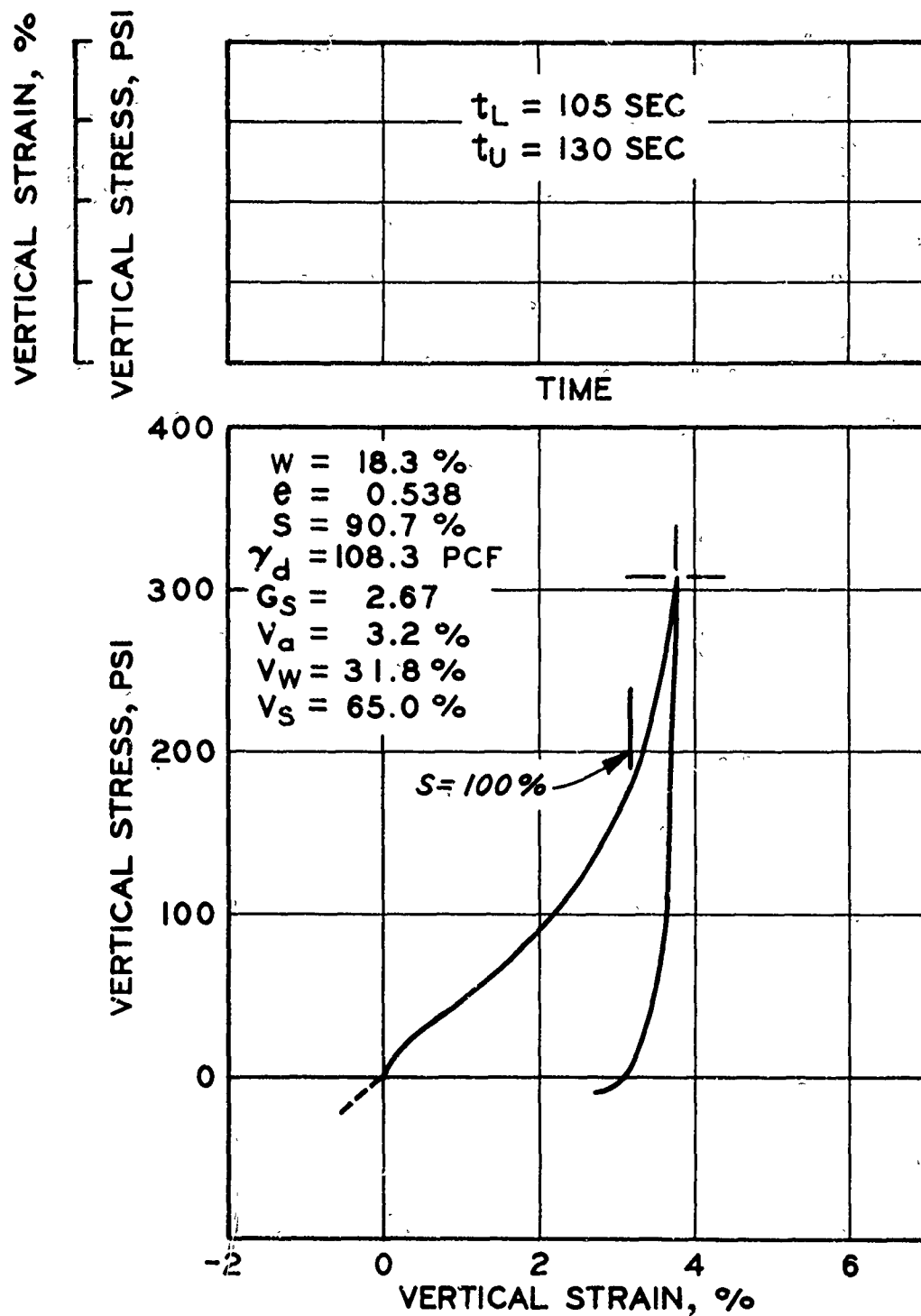


Fig. 1. Static uniaxial strain test HV 5.8.1

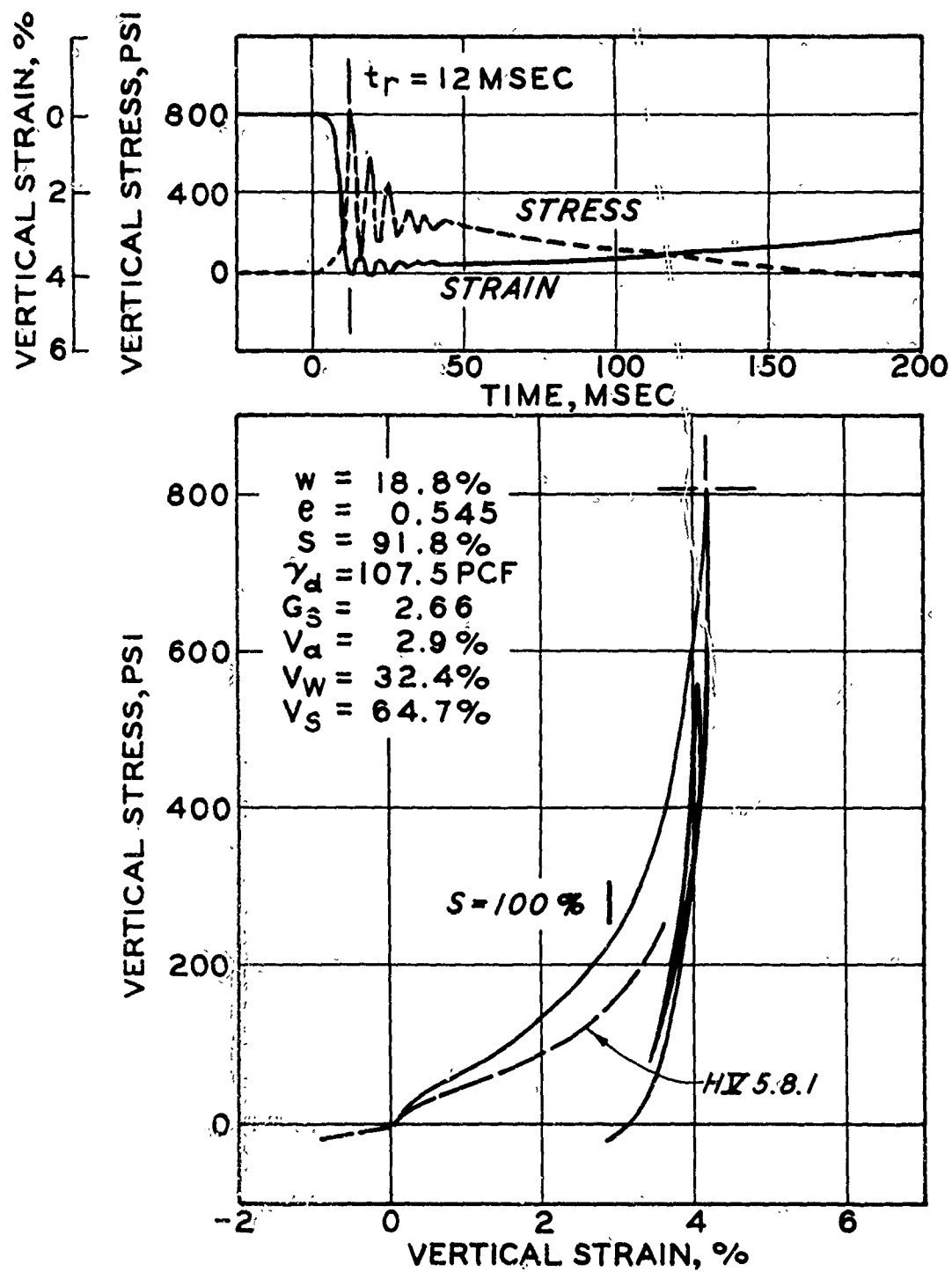


Fig. 2. Dynamic uniaxial strain test HV 5.8.3

vividly the distinct difference between virgin loading and unloading-reloading relations; both need to be defined for computational work. The same phenomena is illustrated in Figure 3 by the results from a test on a sample from Project Backfill near Albuquerque, N. M.

An example of unloading from an initial peak stress level and subsequent reloading to a higher stress level is shown for a North Dakota test specimen in Figure 4. The virgin loading curve is unaffected by this maneuver. Another example can again be found in the Project Backfill results (Figure 5).

Degree of Saturation Effects

Degree of saturation is a factor which can have extreme influences on stress-strain patterns. Tests in support of Operation DISTANT PLAIN on soil samples taken from the Watching Hill test range at the Defence Research Establishment, Suffield (DRES), Canada, provide excellent examples. In Figure 6 are results from a test on a specimen of silty clay with an initial saturation of only 29 percent. Under 1500 psi* the specimen is reduced in volume by 13.5 percent, almost none of which is recovered after unloading. Another silty clay specimen, with almost identical classification and index properties, was obtained some 38 feet below the first one; the only significant difference was that the second specimen was nearly 99 percent saturated. The test results for it are shown in Figure 7. Under 1500 psi it is compressed by only 1.25 percent, almost all of which is recovered after unloading.

Compacted samples of this Suffield silty clay were tested at varying degrees of saturation by Hendron, Davisson, and Parola² (see Figure 8). Increasing water content serves to lubricate the intergranular contacts which results in a substantial lowering of the compression modulus at low pressures. However, the wetter specimens reach 100 percent saturation at lower strains, at which point they "lock" sharply, resulting in a cross over of the stress-strain curves.

Another example of wet soil behavior is shown in Figure 9 for a silty clay specimen obtained from beneath the water table at the HEST Test V site. The specimen compressed only 0.45 percent under 500 psi and the recovery was almost completely elastic.

Unexpected Subsurface Layers

But it is dangerous to assume that all soils found beneath a water

* A table of factors for converting British units of measurement to metric units is presented on page vii.

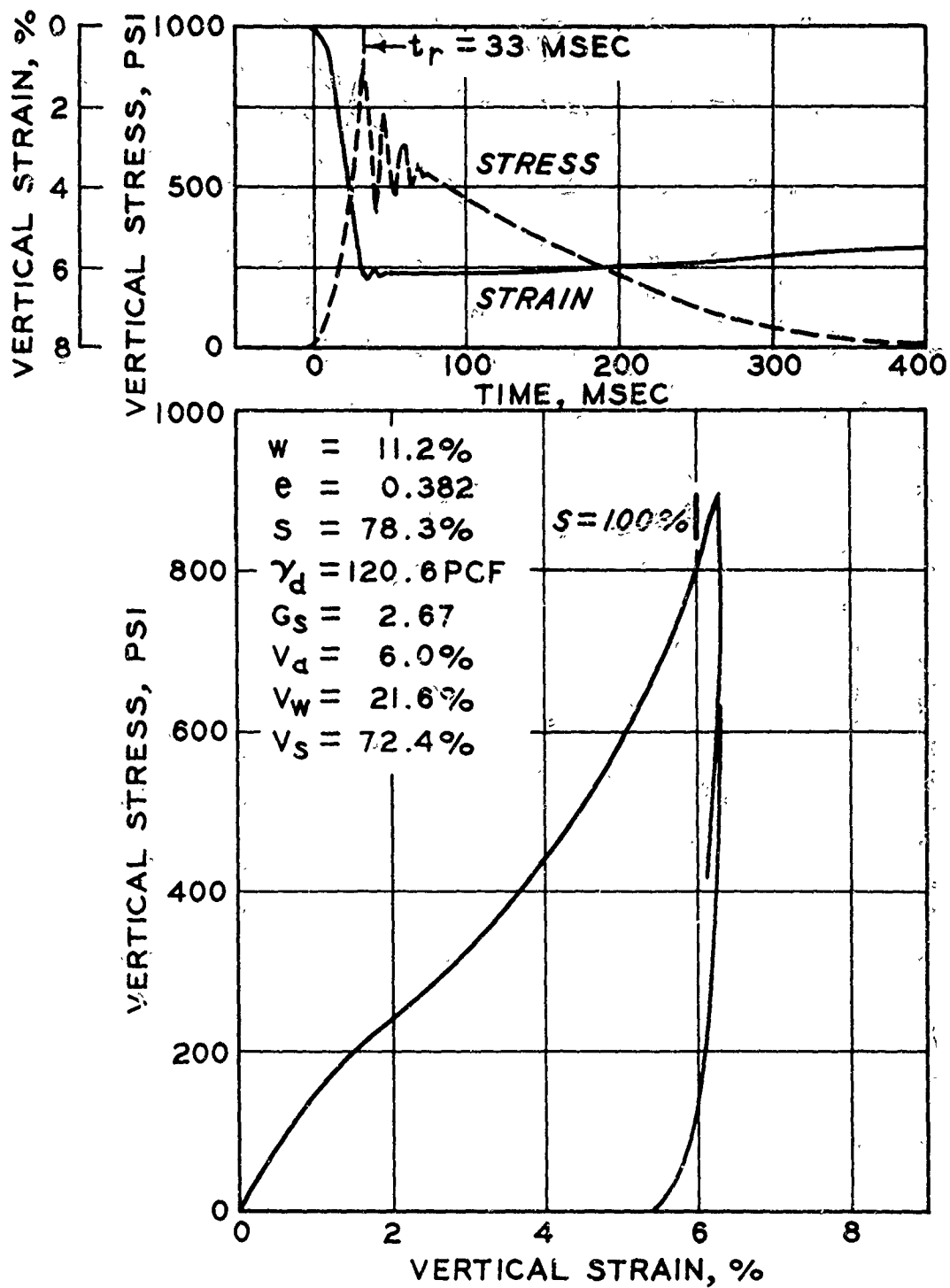


Fig. 3. Dynamic uniaxial strain test BF 2X81

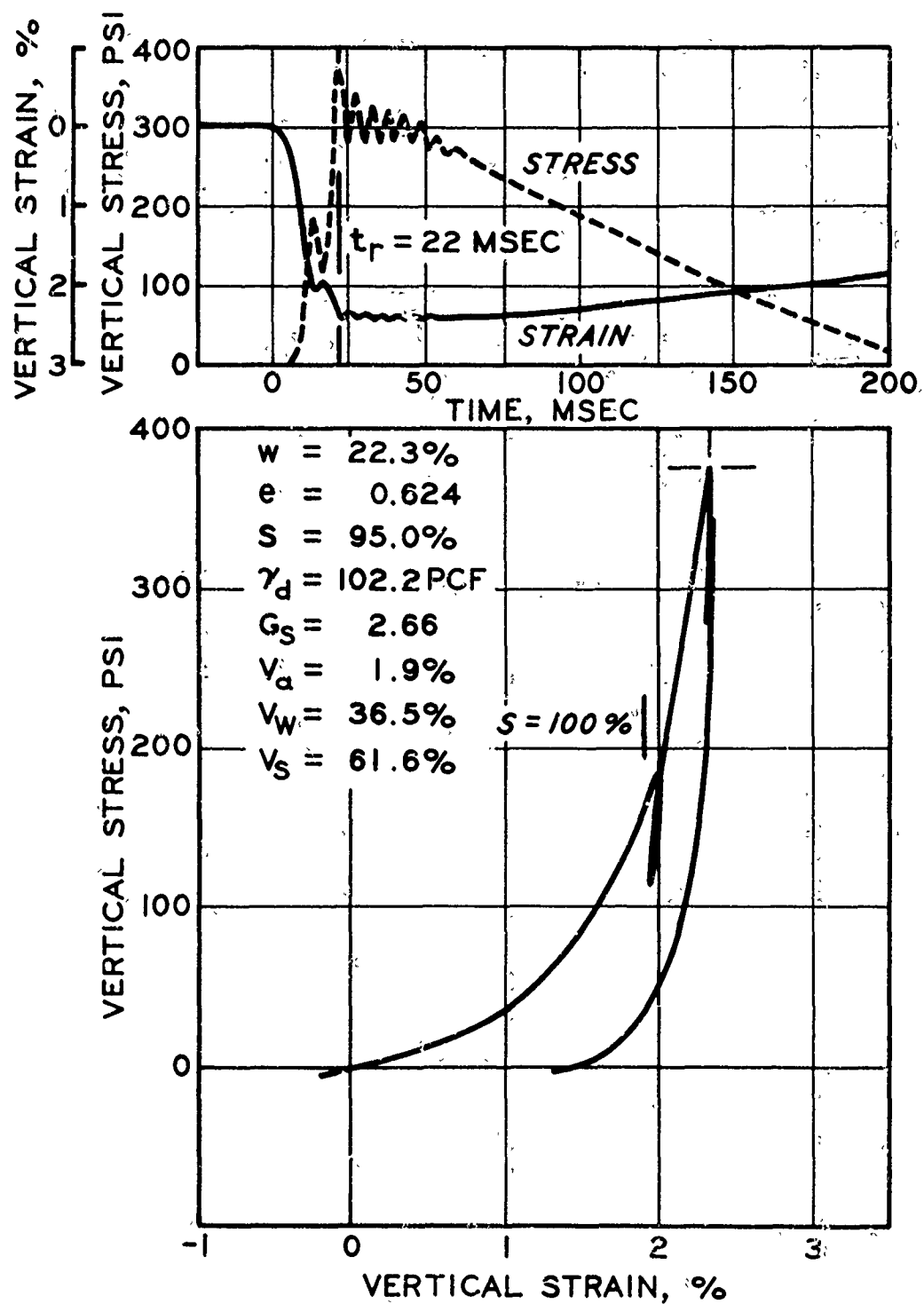


Fig. 4. Dynamic uniaxial strain test HV 4.1.4

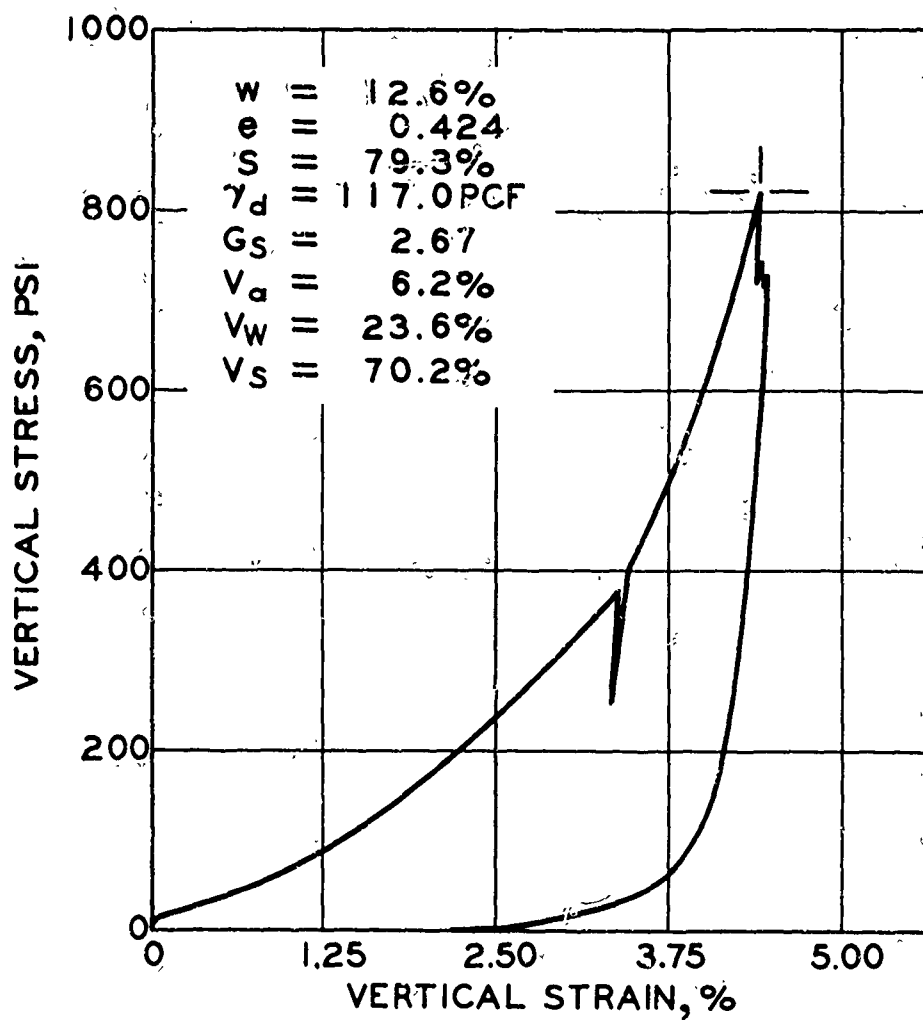
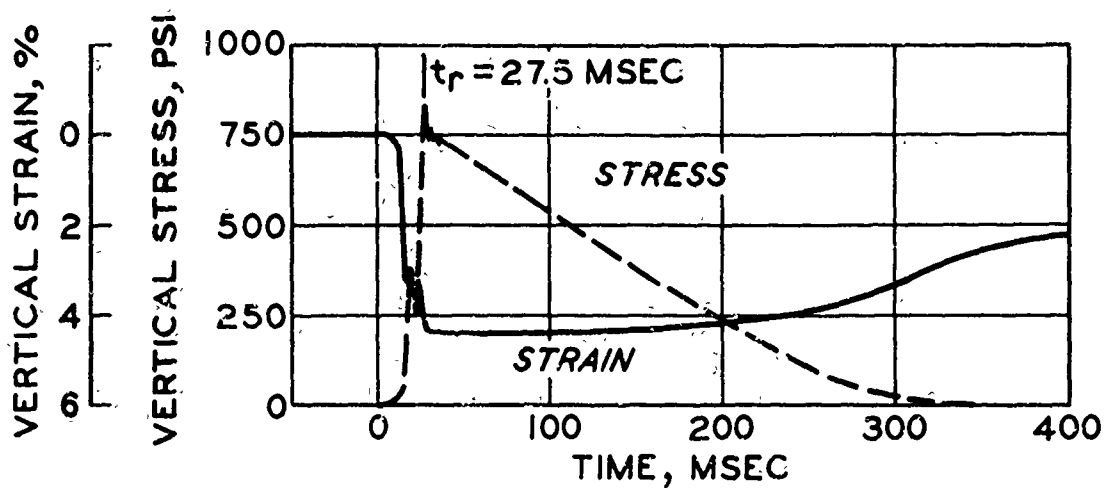


Fig. 5. Dynamic uniaxial strain test BF 5007

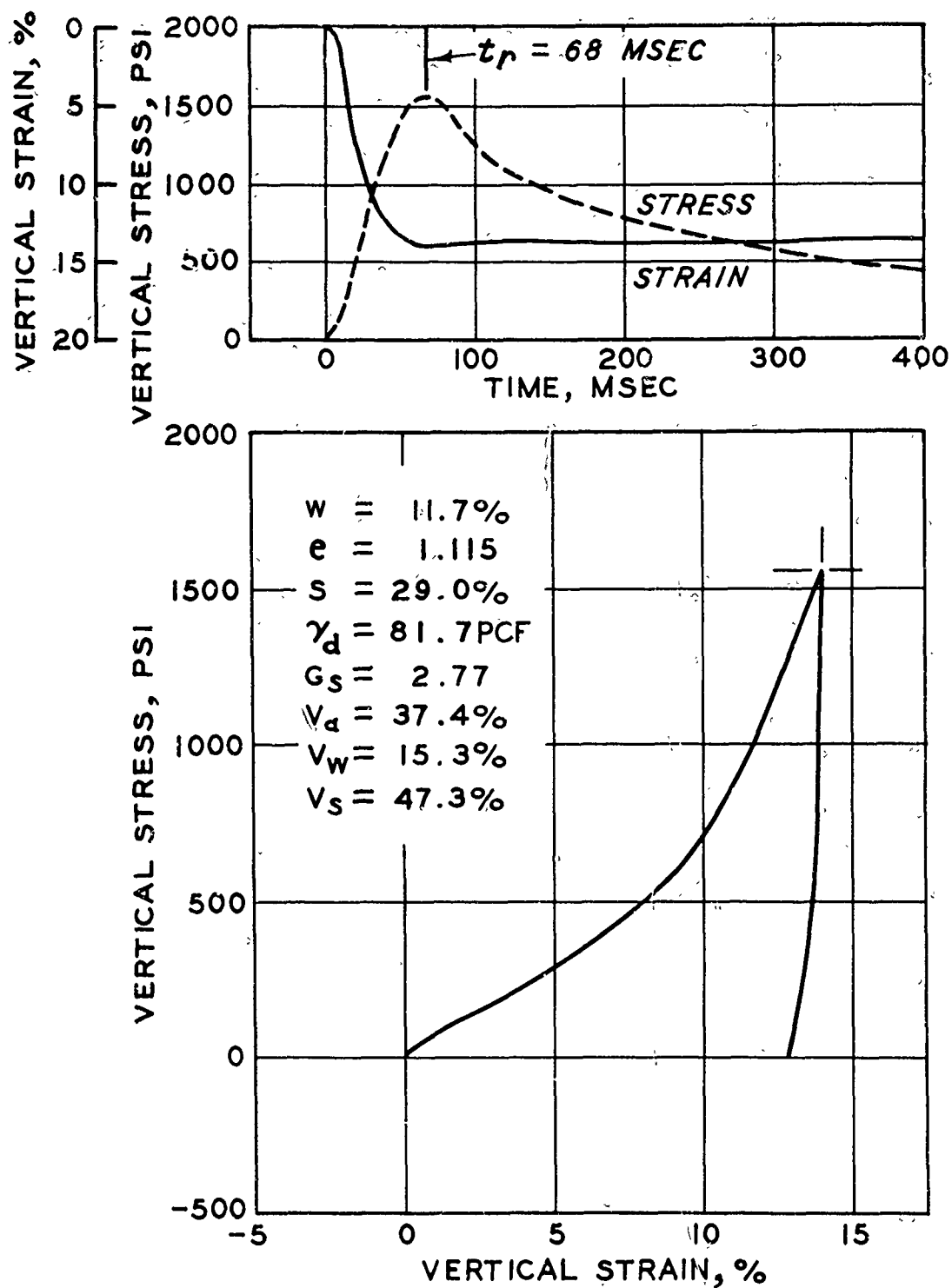


Fig. 6. Dynamic uniaxial strain test DP 1.1.3

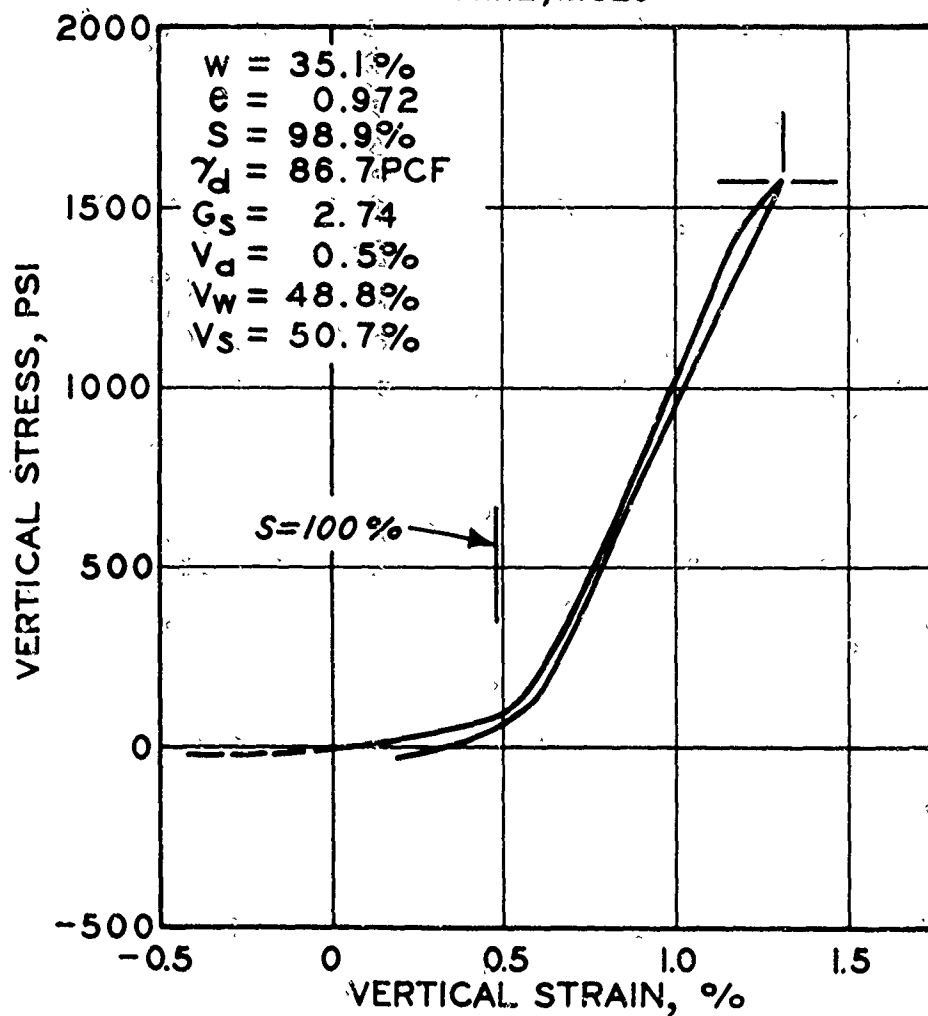
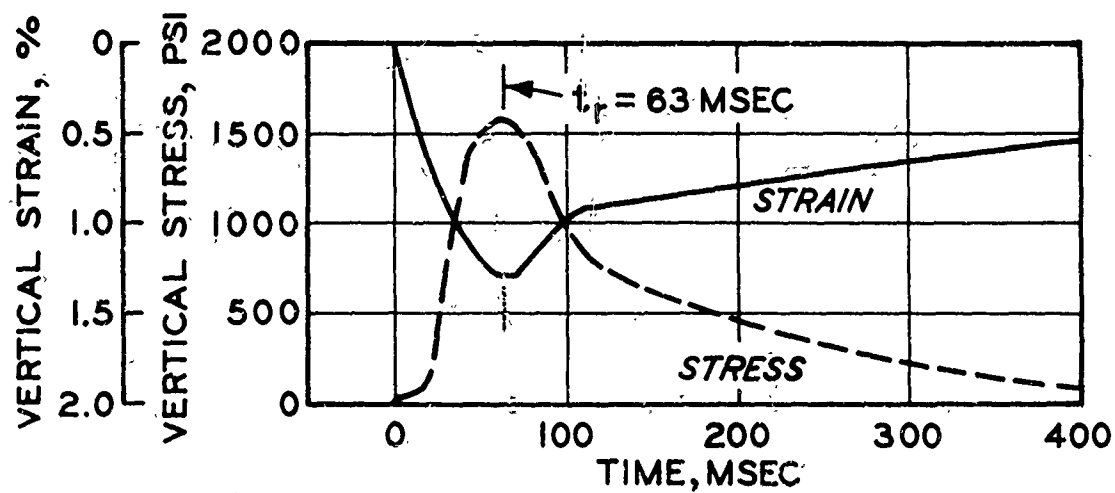


Fig. 7. Dynamic uniaxial strain test DP 3.5.2

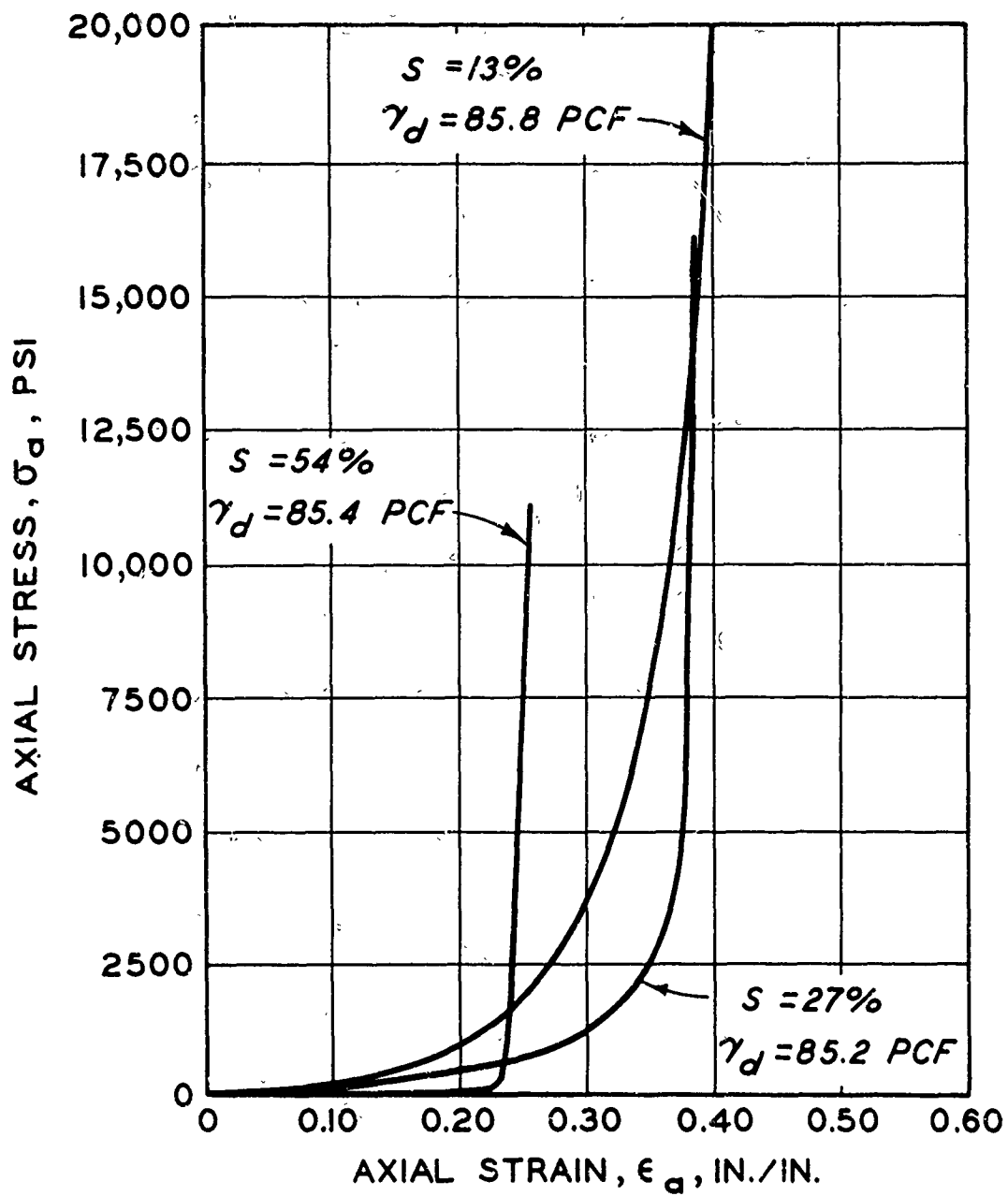


Fig. 8. Stress-strain curves for compacted samples of silty clay (from Hendron, Davisson, and Parola²)

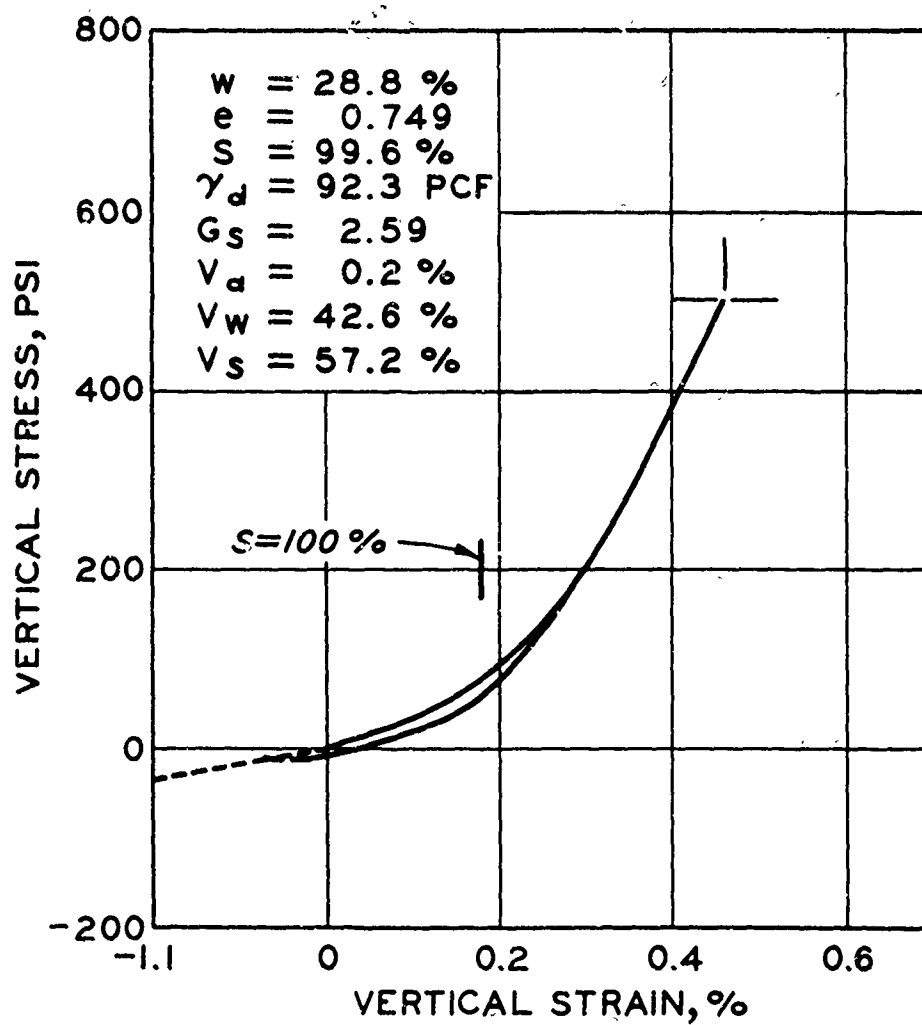
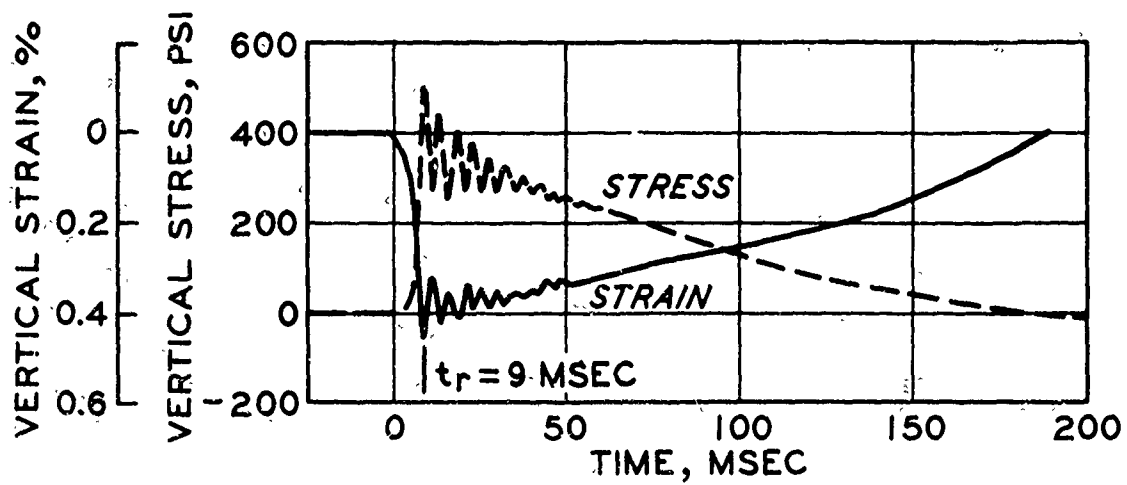


Fig. 9. Dynamic uniaxial strain test HV 5.15.3

table behave like the ones shown in Figures 7 and 9. The test shown in Figure 10 was conducted on specimen No. HV 3.23.2, also obtained at the HEST Test V site, but 31 feet below specimen No. HV 5.15.3 (Figure 9). Strain at a stress of 500 psi was over 2 percent and unloading behavior was certainly not elastic. Subsequent tests were conducted on specimens obtained at the same depths from other borings and the results verified the existence of a compressible underlying stratum. The point being made is that unexpected subsurface layers that will affect ground shock response do exist and can only be found by a careful program of sampling and testing.

Weathering Effects

Simply bringing bags of disturbed soil materials back to the laboratory and preparing remolded test specimens to the estimated in-situ water content and density can produce misleading results since natural processes such as oxidation (or weathering) often alter the soil structure, leading to significant changes in compressibility. Compare the results in Figure 11 for the oxidized specimen No. HV 4.7.4 with the results in Figure 12 for the unoxidized specimen No. HV 4.7.3. The only prior clue that their compression behavior might be different was their color--the oxidized specimen was brown, the unoxidized specimen was gray. All other classification and index properties showed them to be identical--as would their remolded compression behavior, in all probability.

Good undisturbed sampling is a must. It also pays to examine each specimen carefully--specimens Nos. HV 4.7.4 and HV 4.7.3 were obtained from the same 2-1/2-ft.-long Shelby tube which apparently spanned the oxidized-unoxidized interface. The existence of this layer interface in the site profile was also verified by subsequent tests (see Figures 13 and 14).

Geostatic Stress Effects

Another factor influencing constrained modulus is the weight of the overburden above the sample or geostatic stress. These stresses are relieved when the specimen is removed from the ground and should be re-imposed as a static preload prior to application of a live dynamic test load. The unoxidized HEST Test V specimen No. HV 3.7.2 had a static preload of 21 psi; shown with the No. HV 3.7.2 results in Figure 14 are the initial loading portions of the stress-strain curves from two other unoxidized specimens from the same boring, i.e., No. HV 3.20.1 with 57 psi preload and No. HV 3.39.3 with 93 psi preload. Insofar as compressibility--and, hence, wave velocity--is concerned, geostatic overburden stresses have the effect of artificially creating a succession of different materials. For ground shock calculations, this, in essence, means that even uniform soil deposits have to be treated as if they are layered to a certain extent.

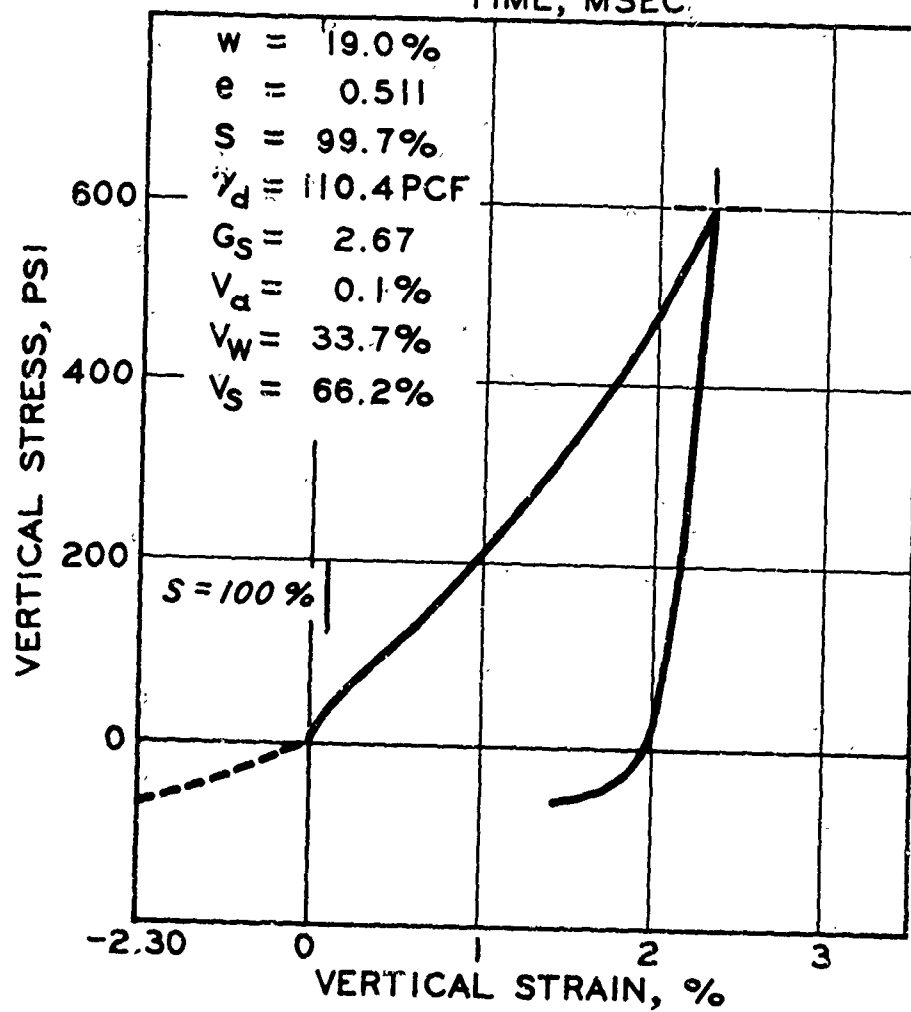
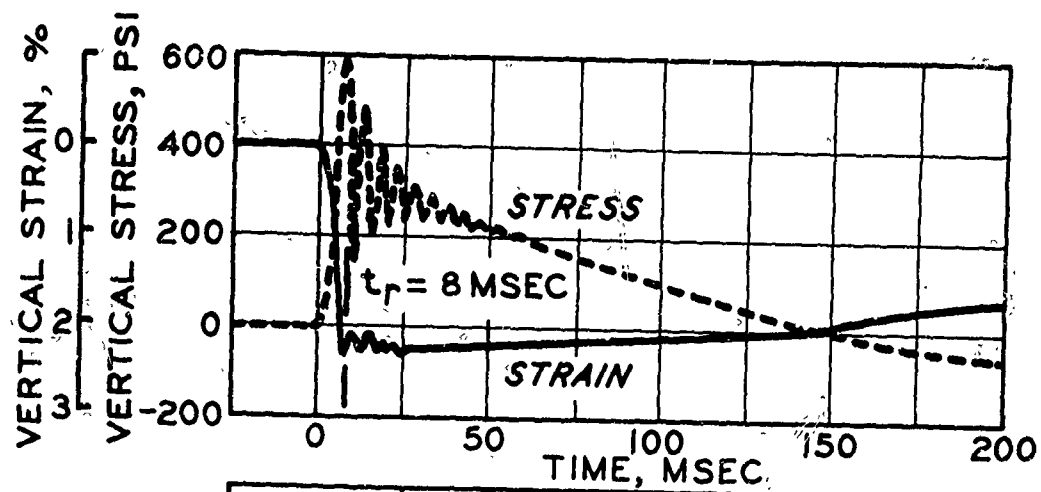


Fig. 10. Dynamic uniaxial strain test HV 3.23.2

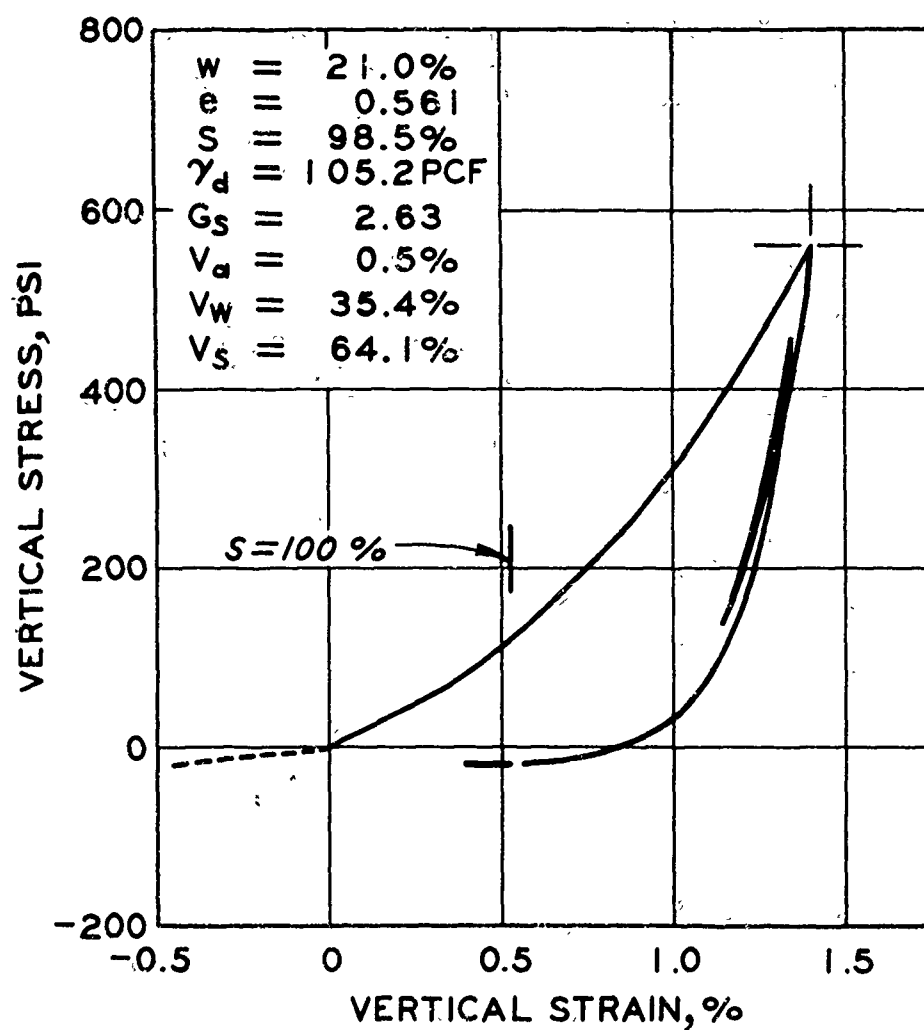
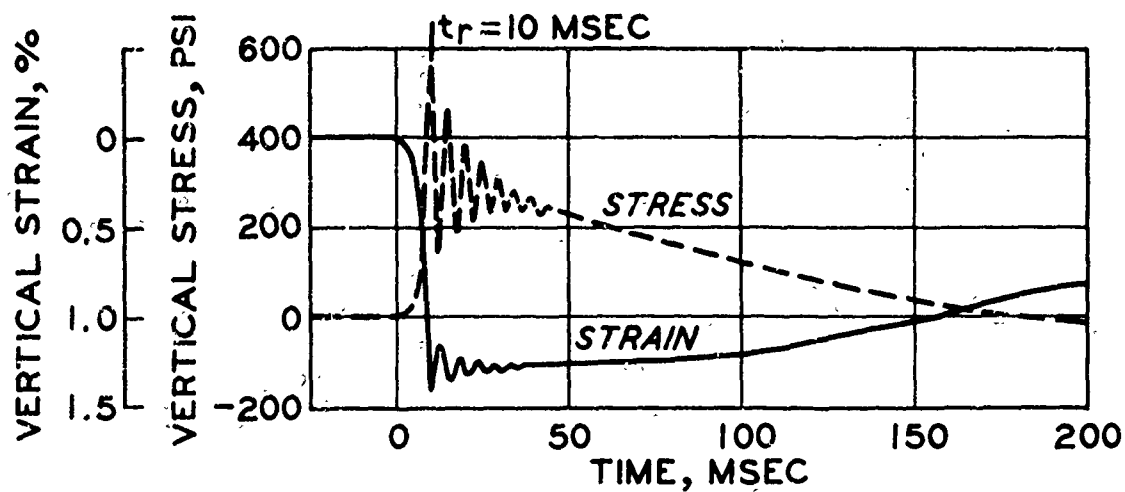


Fig. 11. Dynamic uniaxial strain test HV 4.7.4; brown sandy clay (CL)--oxidized.

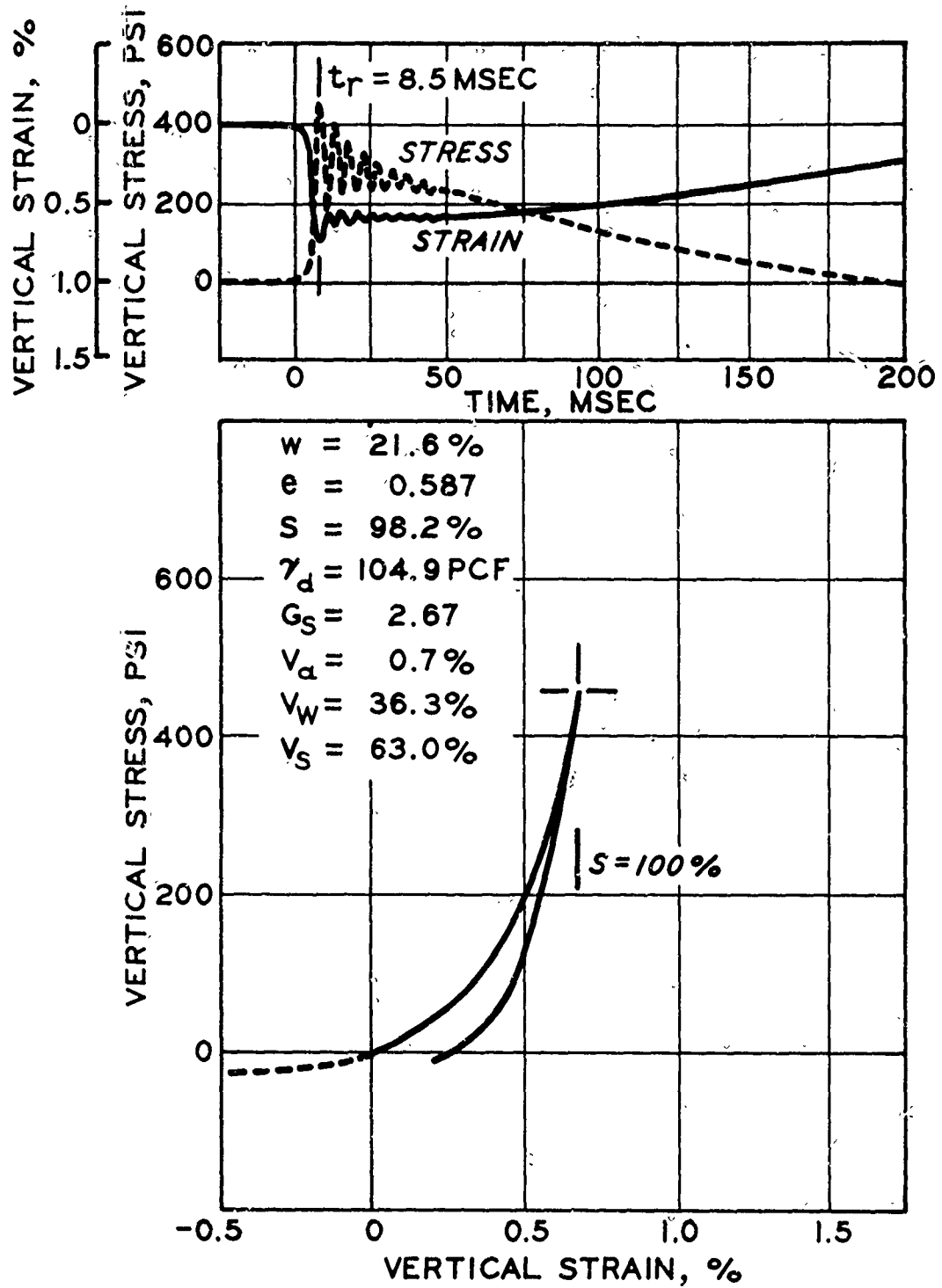


Fig. 12. Dynamic uniaxial strain test HV 4.7.3;
gray sandy clay (CL)--unoxidized

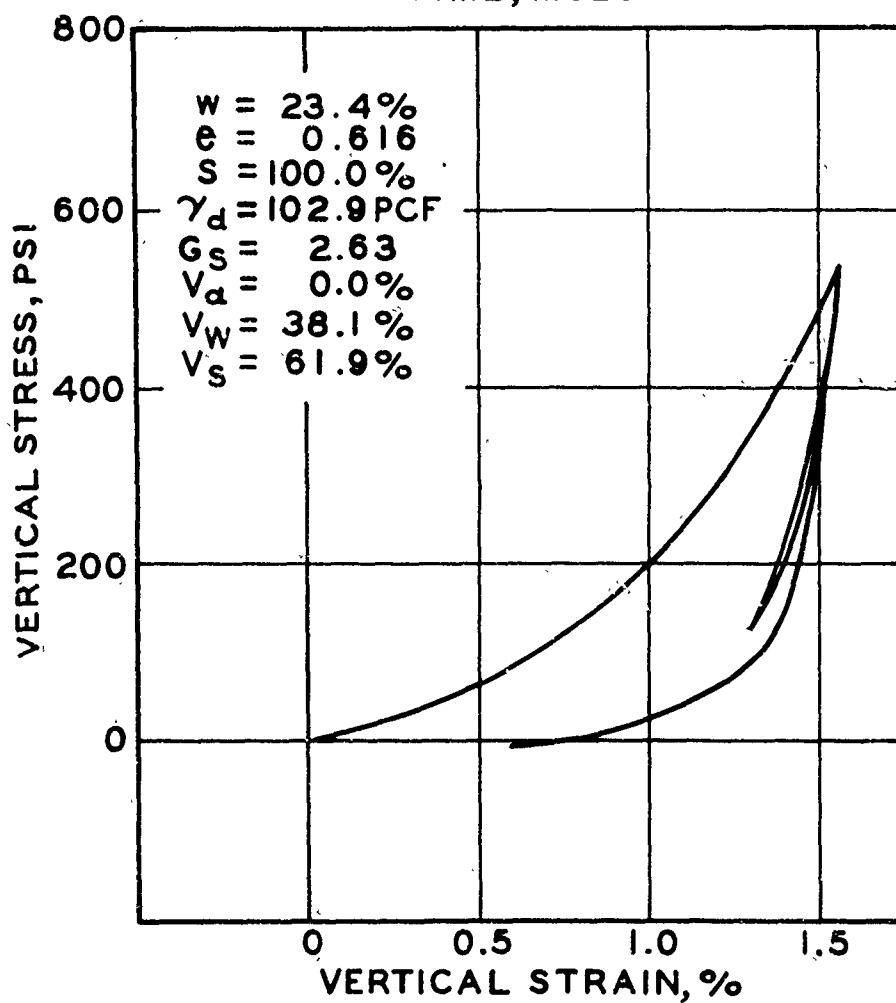
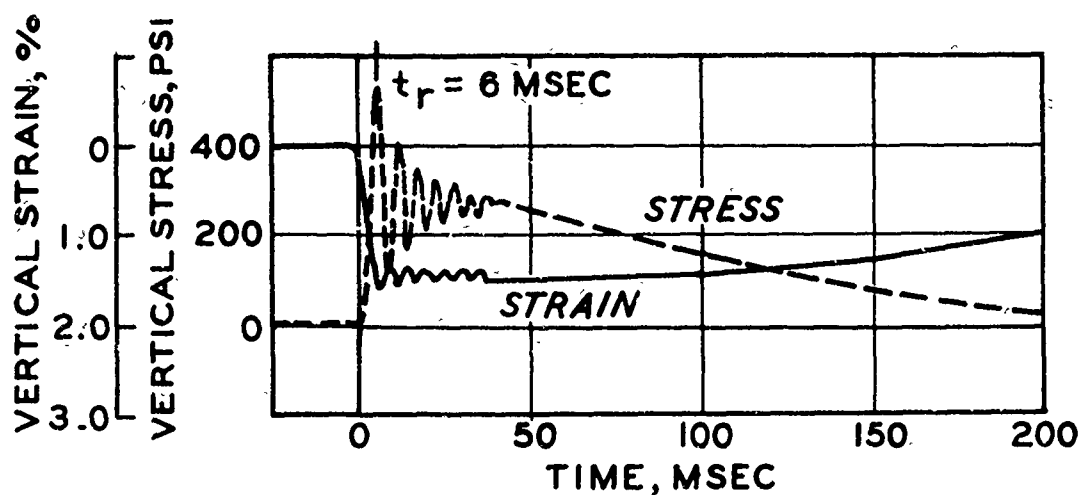


Fig. 13. Dynamic uniaxial strain test HV 3.2.2;
brown sandy clay (CL)--oxidized

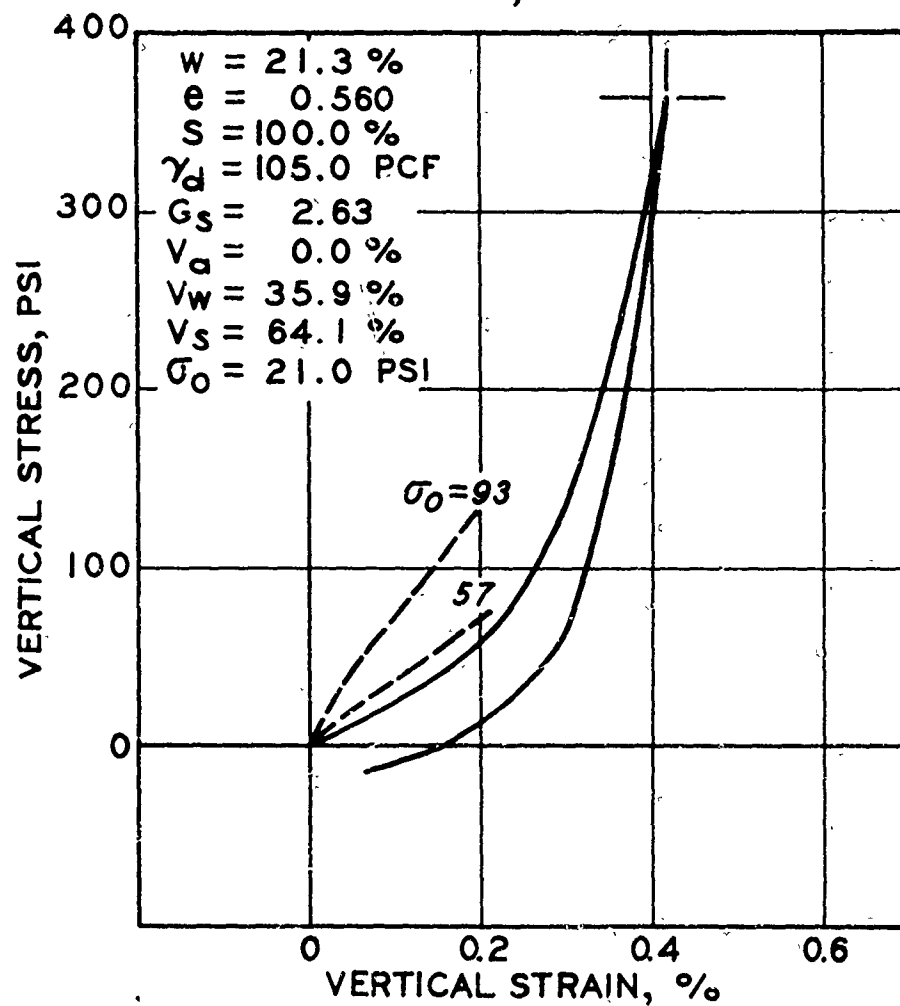
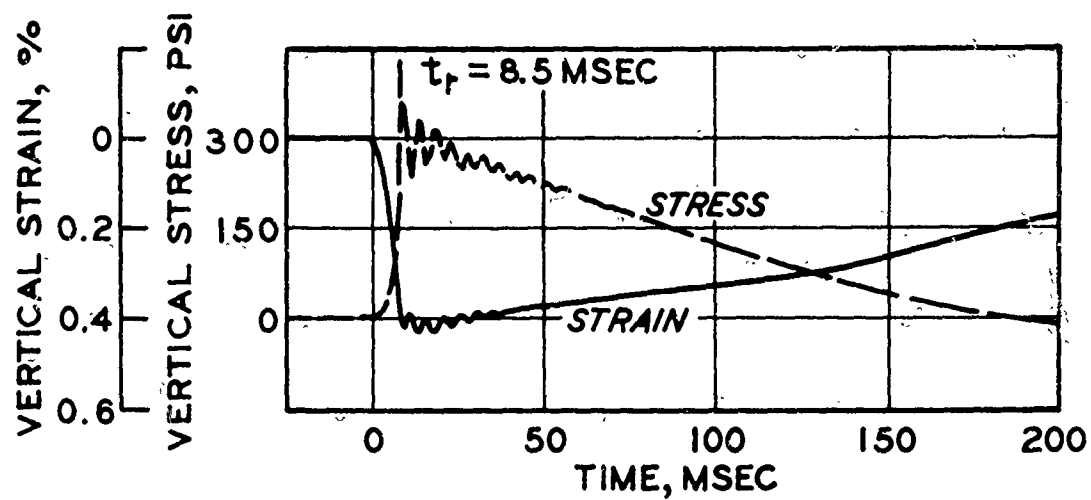


Fig. 14. Dynamic uniaxial strain test HV 3.7.2; gray sandy clay (CL)--unoxidized

Application of Data to Computer Codes

A number of factors which affect the constrained modulus of soils have been discussed. The object of the game, however, is to incorporate the constrained modulus data into a constitutive equation that can be used in a computer code for calculating ground shock response for a given problem.

For one-dimensional problems, a simple linear-hysteretic model is sometimes used where

$$\sigma = M_L \epsilon \text{ during virgin loading}$$

$$\sigma = M_u \epsilon \text{ during unloading-reloading}$$

in order to properly account for oscillations (both real and code-induced) in the stress histories being computed, code logic must be based on both the total stress history (i.e., memory of previous maximum strain) and the direction of the stress change (i.e., sign of the strain increment change associated with the current time-step) at each calculation node point. An example of the effect on the stress-strain relation of omitting monitorship of previous maximum strain is given in Figure 15 for a linear-hysteretic model subjected to oscillatory stress. This incorrect logic will overdamp the calculated output.

The next obvious step is a nonlinear-hysteretic model where M_L and M_u are nonlinear functions of stress or strain. Such functions often take the form of polynomials fitted to experimental data. An example of such a fit to a virgin loading curve used to describe one of the soil layers at the DISTANT PLAIN site is given in Figure 16.

Unloading-reloading curves can also be fit with polynomials but with considerably more difficulty. Unlike the case of a virgin loading curve where a single equation can be used, description of unloading-reloading requires a family of equations. Thus, the form of the polynomial fit becomes important. Several possible forms are shown in Figure 17 along with the family of curves each would generate if fitted to the given experimental unloading-reloading relation. Figures 17(a) and 17(b) illustrate relatively simple linear translation of curve segments to the point of unloading--neither produces a family of curves that is characteristic of real behavior. From the standpoint of producing realistic-looking curves, the dimensionless form shown in Figure 17(c) which preserves the complete curve shape regardless of the point of initial unloading, is certainly preferable. The usually long and extremely steep slope followed by a sharp breaking "tail" that characterizes experimental unloading curves is difficult to fit and the many roots in the equation solution cause logic headaches that may not be worth the effort--a curve consisting of several linear segments would probably be satisfactory.

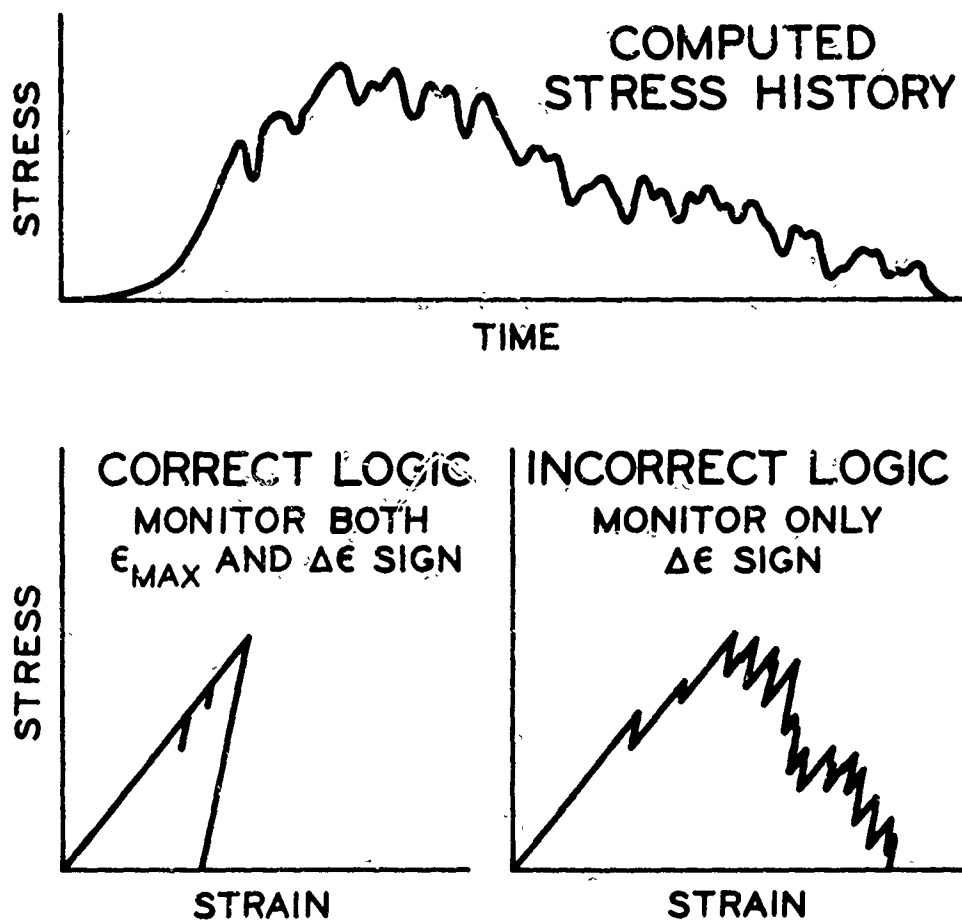


Fig. 15. Effect on stress-strain relation of omitting monitorship of ϵ_{max}

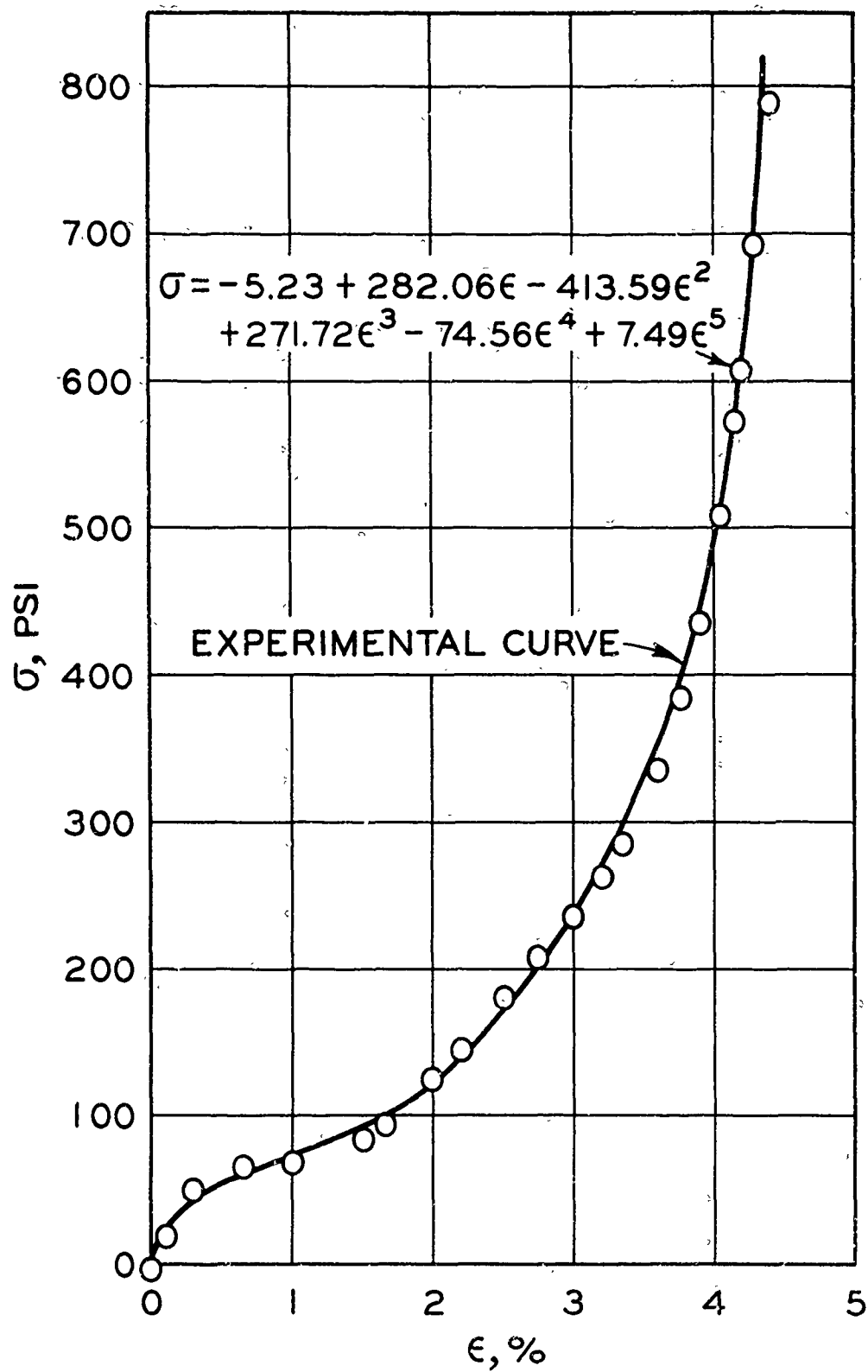


Fig. 16. Polynomial fit to virgin loading curve

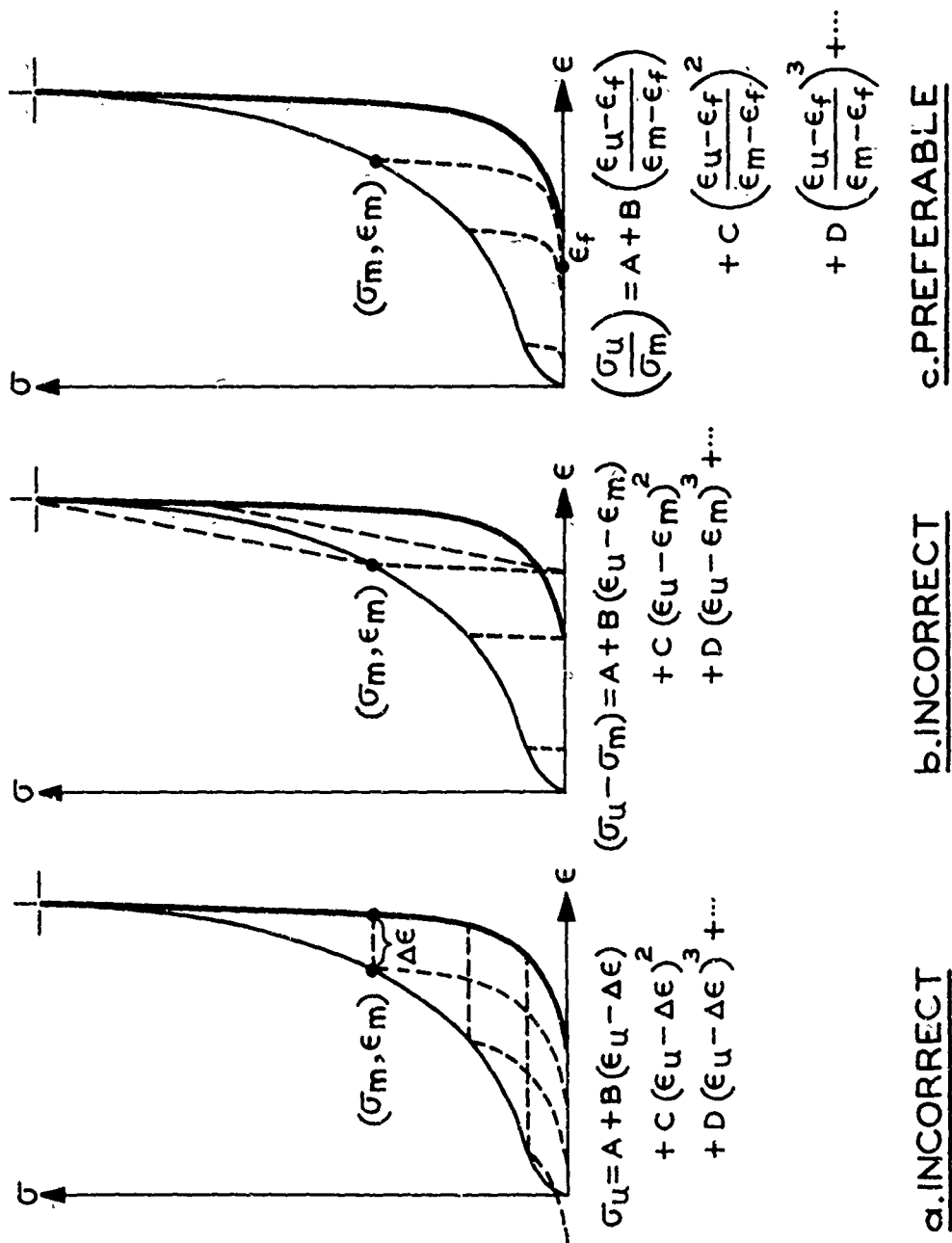


Fig. 17. Polynomial forms for unloading-reloading equations

Two-dimensional problems involve not only vertical stresses and motions but also radial or lateral response. Thus, as inferred in the introduction, constrained modulus data is not sufficient in itself to describe the tensor constitutive relationship necessary for such calculations. However, if radial stresses are measured during the uniaxial strain test, then other modulus data can be calculated.

Figure 18 shows an example of the results from a static uniaxial strain test with radial stress measurements by Davisson and Maynard³ on an undisturbed specimen of Suffield silty clay. Notice that the axial stress-radial stress relations are different for loading and unloading. Bulk modulus (K) and shear modulus (G) curves can be calculated from this data as indicated in Figure 19. The most striking aspect of these plots is their similarity of form. Hendron, Davisson, and Parola² statically tested remolded specimens of the Suffield silty clay up to 20,000 psi (Figure 20). K and G curves were also calculated for this test as shown in Figure 21.

TRIAXIAL COMPRESSION TEST RESULTS

Current use of the triaxial compression test is primarily aimed at determining the ultimate strength or limiting conditions for shear failure with a soil mass. A cylindrical sample is first subjected to an all-around confining pressure; this confining pressure is then held constant while the specimen is strained axially under an increasing axial stress until shear failure occurs. Radial strains are generally not measured. The result of each test is a plot of principal stress difference ($\sigma_a - \sigma_r$) versus axial strain (ϵ_a). A series of tests must be conducted, each at a different confining pressure and each ideally on identical specimens, in order to construct a Mohr shear strength envelope depicting shearing stress acting on a failure plane as a function of the normal stress acting on the same plane. Each envelope is described by a friction angle, ϕ , and a cohesion intercept, c .

Shear Strength Data

An example of the results from a series of dynamic unconsolidated-undrained triaxial compression tests conducted on saturated clay specimens from the DISTANT PLAIN test site is given in Figure 22. Note that the curves are relatively independent of confining pressure and that the resulting Mohr envelope is flat, i.e., $\phi = 0$. This is characteristic of saturated clays; in theory of plasticity such shear behavior is characteristic of von Mises materials.

An example of results from a similar series conducted on partially saturated sandy clay specimens from the HEST Test V site is given in Figure 23. In this case, the curves are quite obviously functions of confining pressure and the Mohr envelope has both a cohesive intercept

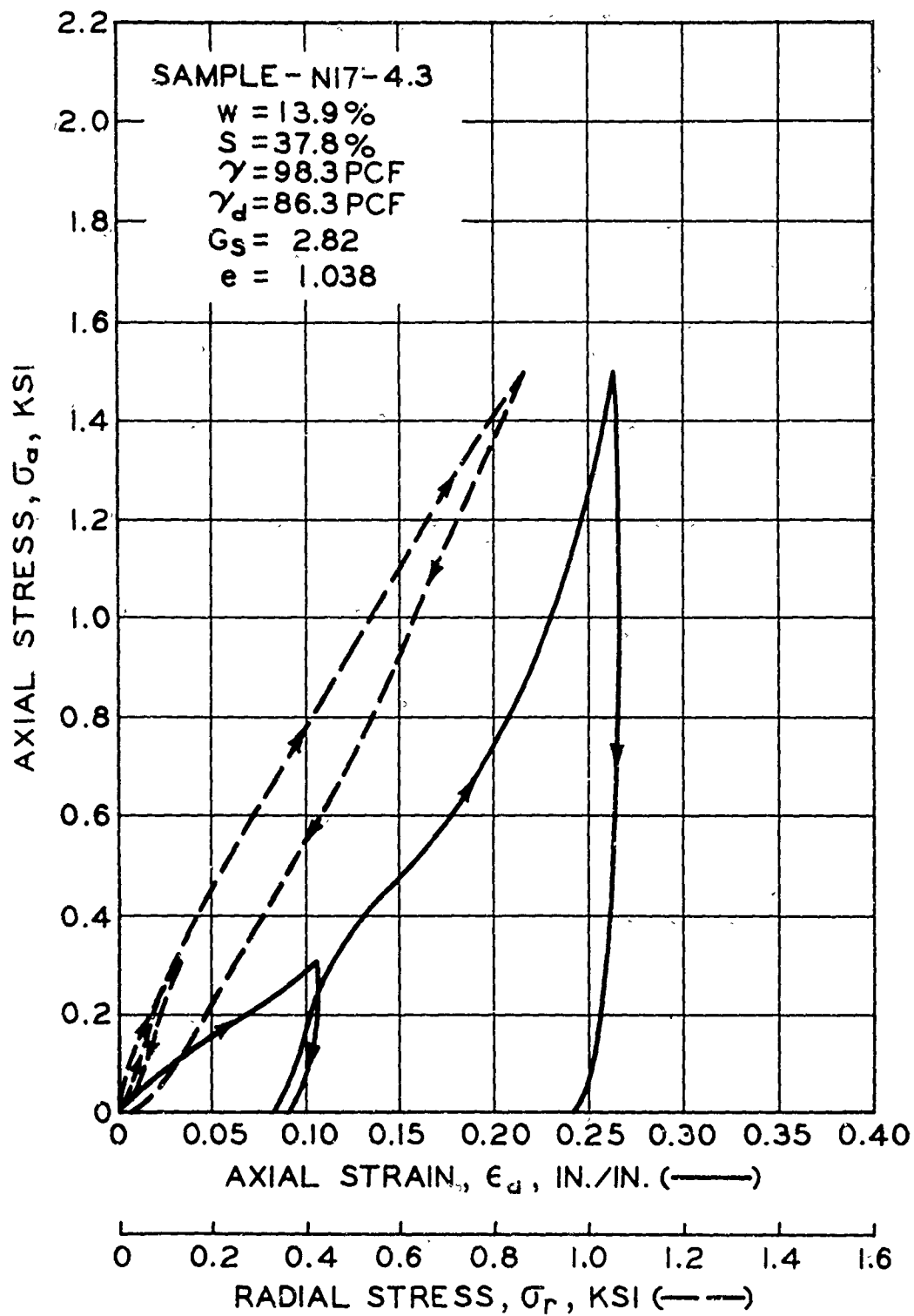


Fig. 18. Uniaxial strain test on Suffield silty clay
 (from Davisson and Maynard³)

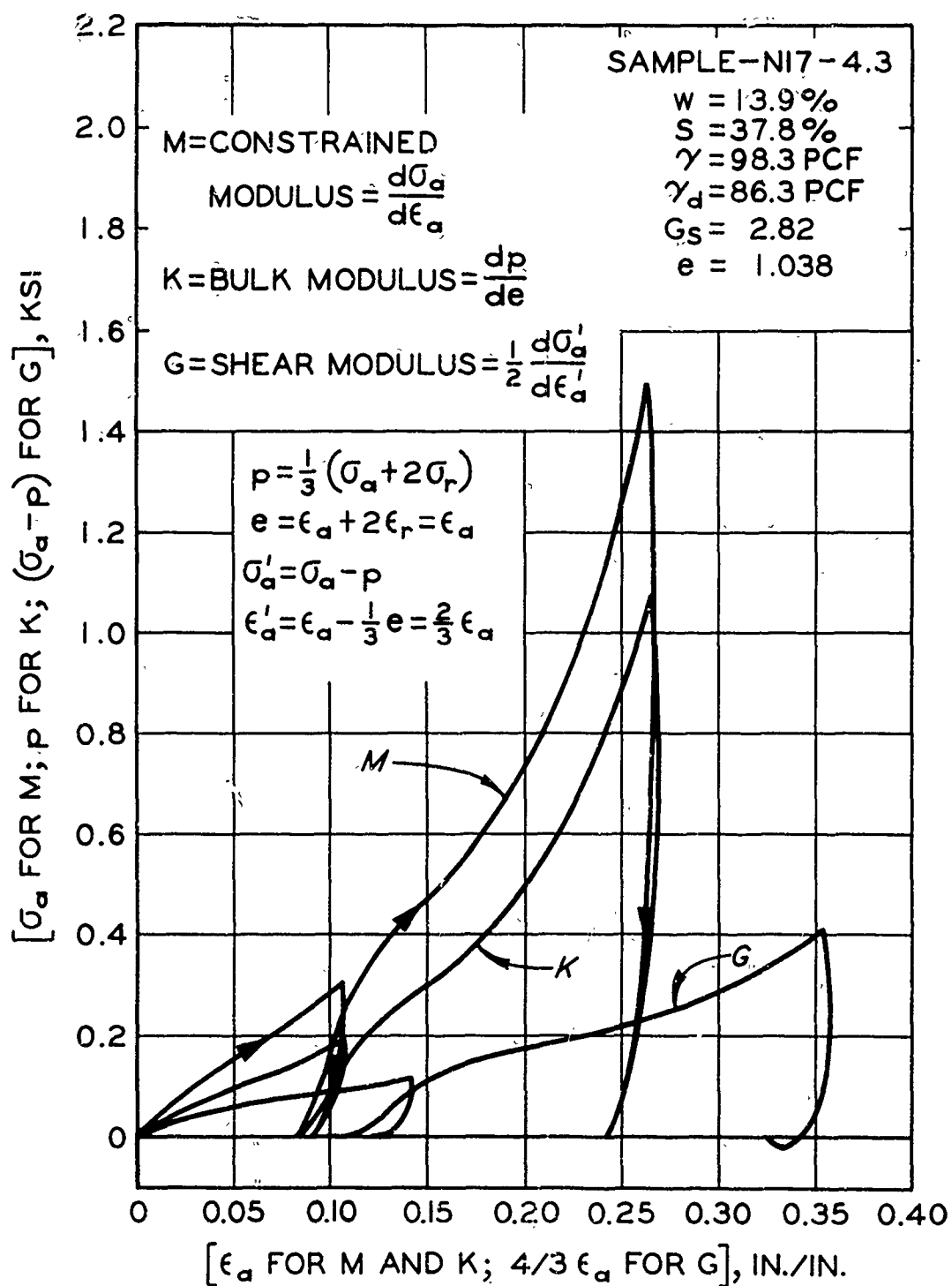


Fig. 19. Stress-strain relations from uniaxial strain test
(from Davisson and Maynard³)

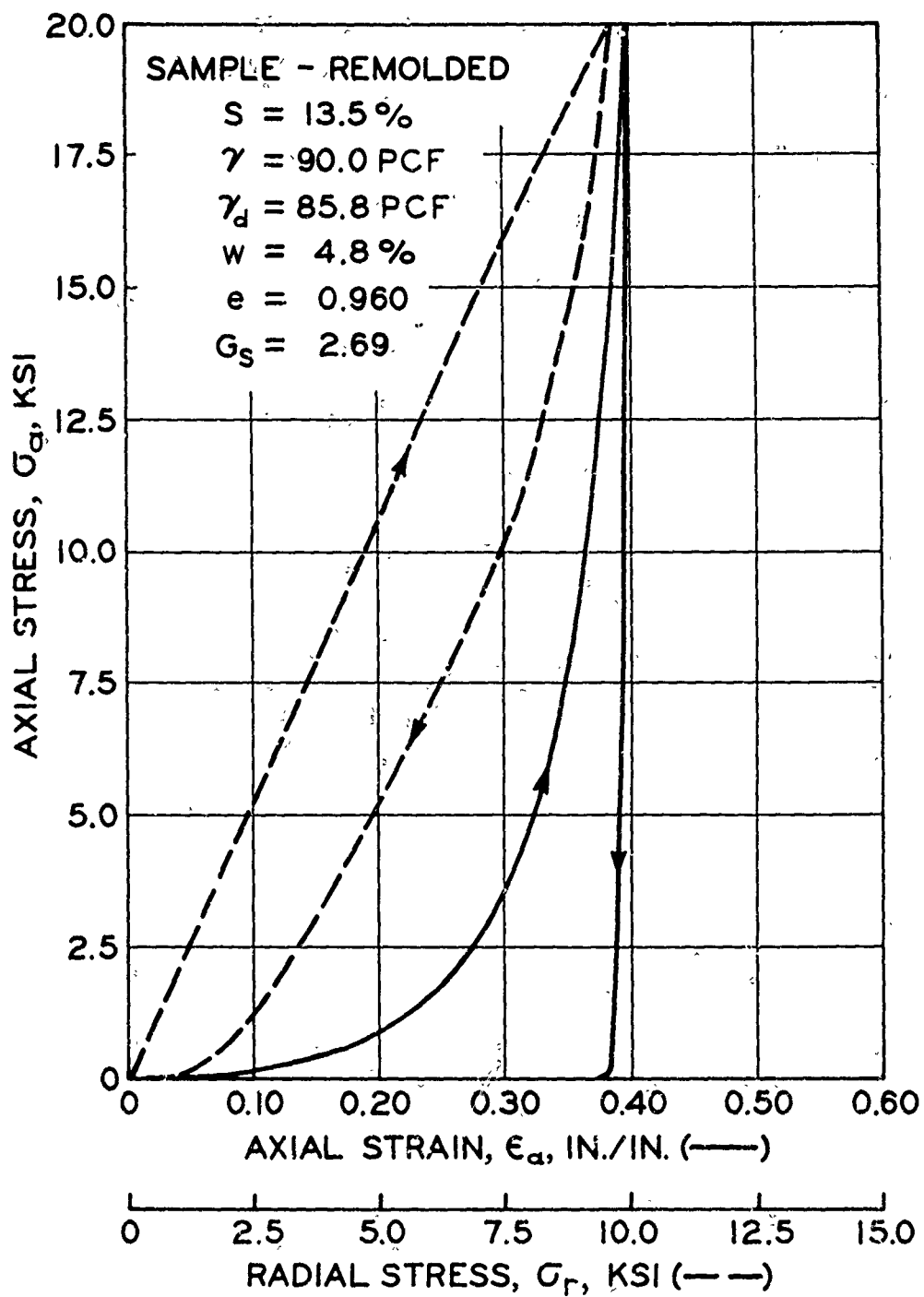


Fig. 20. Uniaxial strain test on Suffield silty clay
 (from Hendron, Davisson, and Parola²)

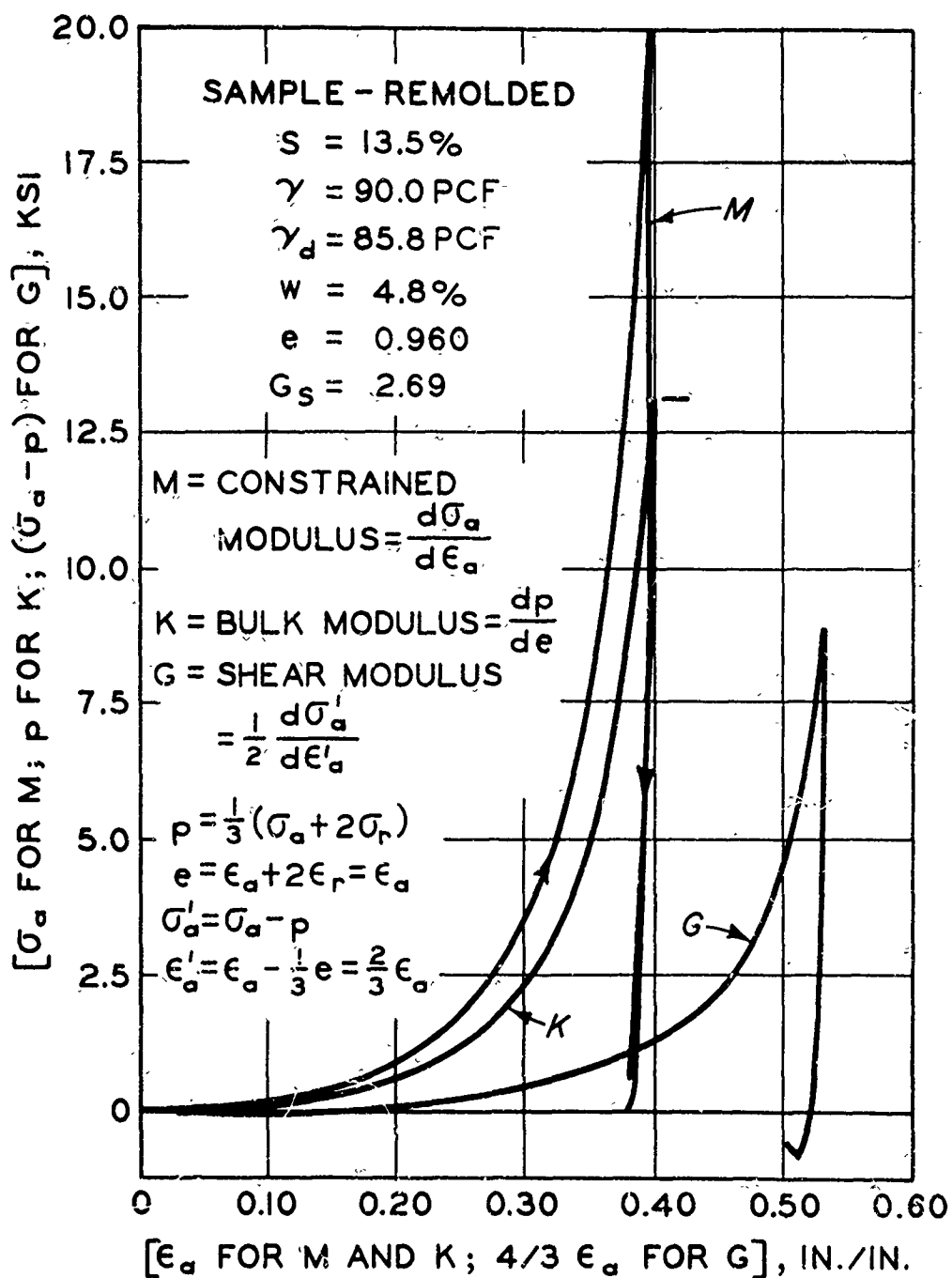


Fig. 21. Stress-strain relations from uniaxial strain test
(from Hendron, Davisson, and Parola²)

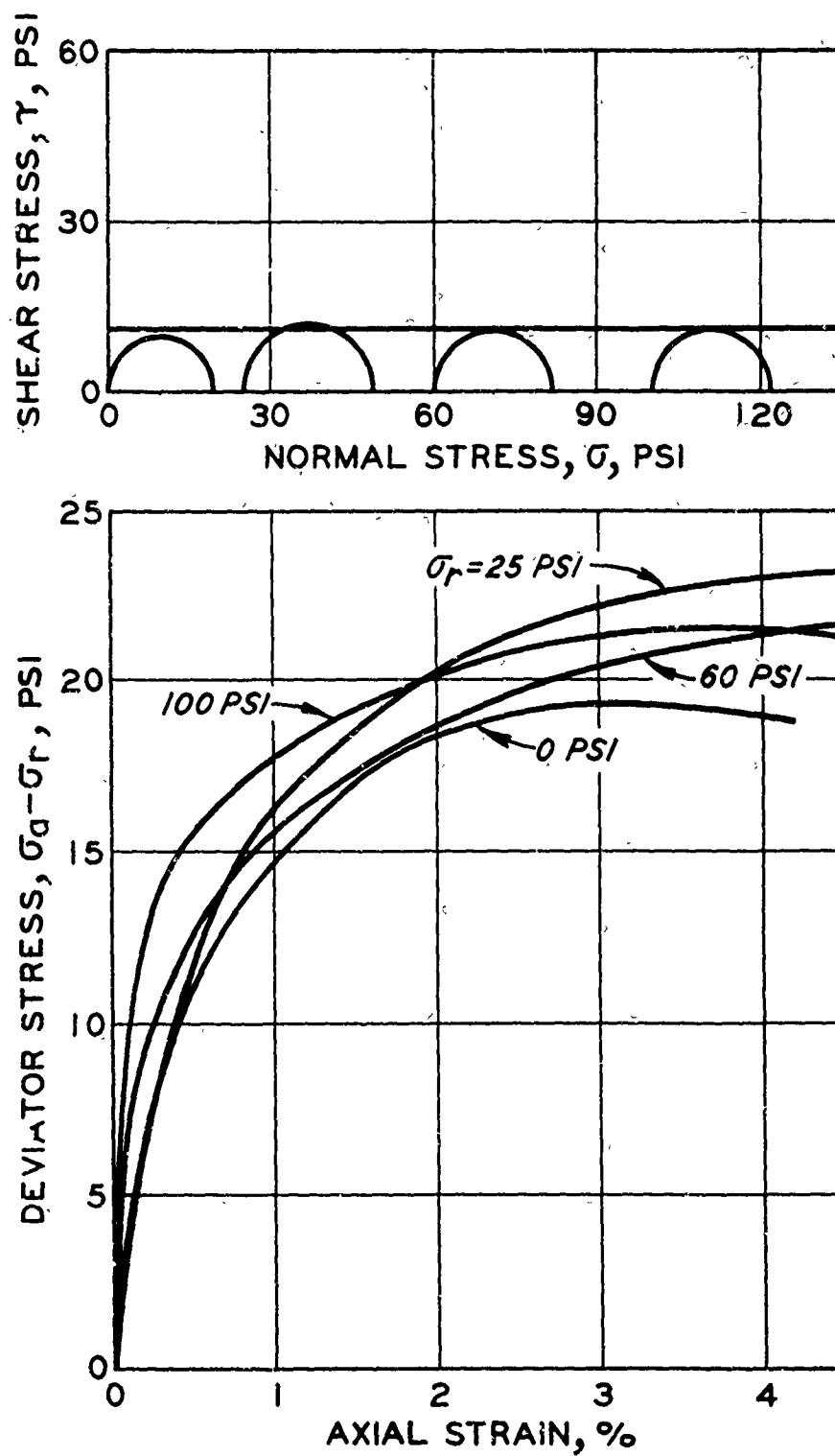


Fig. 22. Dynamic triaxial compression series DP 6.3.0

and, at least initially, a definite friction angle. Soils exhibiting this type behavior are related to the Coulomb (with cohesion) model of plasticity theory. At the higher confining pressures, specimen saturation increases causing the envelope to flatten (or approach the von Mises yield condition) as the pore water carries more and more of the applied normal stress. This effect is evident in the results shown in Figure 23 and was verified by results from a companion specimen tested statically by Mazanti and Holland⁴ under a confining pressure of 980 psi.

Yield Criteria for Computer Codes

Most computer codes that attempt to account for plastic behavior incorporate a yield condition based on the three-dimensional generalization by Prager-Drucker

$$\sqrt{J_2'} = k + \alpha J_1 = k + 3\alpha p$$

where

$$J_2' = \text{second invariant of stress deviation} = \frac{1}{2} \sigma_{ij}' \sigma_{ij}'$$

$$J_1 = \text{first invariant of total stress} = \sigma_{11} + \sigma_{22} + \sigma_{33}$$

$$p = \text{mean normal stress} = 1/3 J_1$$

k & α = material coefficients

For the triaxial compression test

$$\sqrt{J_2'} = \frac{\sigma_a - \sigma_r}{\sqrt{3}}$$

$$p = \frac{\sigma_a + 2\sigma_r}{3}$$

Thus, k and α can be determined directly from the equation of a straight line fitted to a plot of $\sqrt{J_2'}$ versus p . If the input data are c and ϕ from a Mohr diagram, then k and α are computed (for compression positive sign convention) from

$$k = \frac{6 c \cos \phi}{\sqrt{3} (3 - \sin \phi)} \quad \alpha = \frac{2 \sin \phi}{\sqrt{3} (3 - \sin \phi)}$$

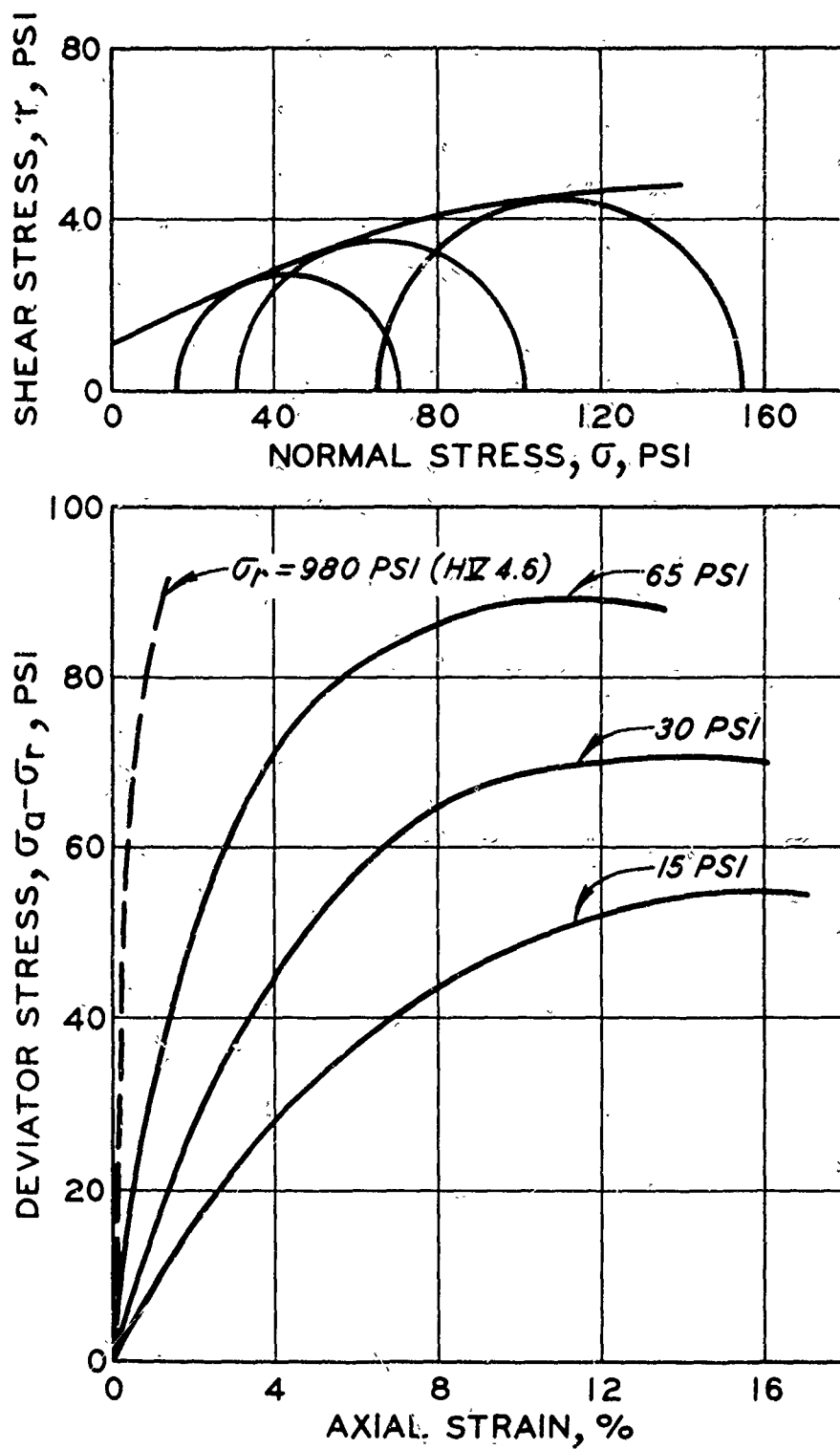


Fig. 23. Dynamic triaxial compression series HV 4.5

If a straight line fit is not practical (as for the data shown in Figure 23), then the computer should be programmed to accept $\sqrt{J_2}$ as some nonlinear function of p .

Stress-Strain Data

In addition to providing data on the ultimate strength or shear resistance associated with failure of the soil specimen, triaxial compression tests do provide some stress-strain information. Young's modulus of elasticity, E , can theoretically be obtained from the stress-strain curve from an unconfined compression test, i.e.,

$$E = \frac{d\sigma_a}{d\epsilon_a} \text{ for } \sigma_r = 0$$

Poisson's ratio, ν , can also be determined from an unconfined test where ν is the ratio between radial strain, ϵ_r , and axial strain, ϵ_a .

However, if radial strains can be satisfactorily measured, then more meaningful data such as bulk modulus, K , and shear modulus, G , can be determined directly from confined triaxial compression tests (i.e., $\sigma_r \neq 0$). Incremental application of the all-around confining pressure, with sufficient strain measurements being made to permit calculation of volume changes, provides a hydrostatic compression test from which bulk modulus data can be obtained. Two examples of this type hydrostatic compression test (by Mazanti and Holland⁴ on the HEST Test V soil) are shown in Figure 24. Even though both curves are quite nonlinear, they exhibit very little hysteresis or inelastic behavior; this is in contrast to the extreme inelastic behavior noted in the K curves calculated from uniaxial strain tests (Figures 19 and 21).

After application of the hydrostatic pressure, shear modulus data can be obtained while the specimen is maintained in a state of constant lateral stress. Examples of this are given in Figure 25 for the two specimens tested by Mazanti and Holland. As expected, they exhibit extreme inelastic behavior but the virgin loading curves are continuously concave to the strain axis--this is in direct contrast to the curvature of the uniaxial-strain calculated G curves (Figures 19 and 21).

CONCLUSION

Laboratory uniaxial strain and triaxial compression test data have been presented to illustrate the effects of various factors such as loading rate, history of unloading-reloading, degree of saturation, weathering, geostatic stress and confining pressure on the stress-strain and strength properties used in soil constitutive relations.

Unclassified

Security Classification

DOCUMENT CONTROL DATA - R & D		
(Security classification of title, body of abstract and indexing annotation must be entered when the overall report is classified)		
1. ORIGINATING ACTIVITY (Corporate author) U. S. Army Engineer Waterways Experiment Station Vicksburg, Mississippi		2a. REPORT SECURITY CLASSIFICATION
		2b. GROUP
3. REPORT TITLE FACTORS THAT INFLUENCE THE DEVELOPMENT OF SOIL CONSTITUTIVE RELATIONS		
4. DESCRIPTIVE NOTES (Type of report and inclusive dates) Final report		
5. AUTHOR(S) (First name, middle initial, last name) John G. Jackson, Jr.		
6. REPORT DATE July 1968	7a. TOTAL NO. OF PAGES 39	7b. NO. OF REFS ---
8a. CONTRACT OR GRANT NO.	8b. ORIGINATOR'S REPORT NUMBER(S) Miscellaneous Paper No. 4-980	
b. PROJECT NO.		
c.	9b. OTHER REPORT NO(S) (Any other numbers that may be assigned this report)	
d.		
10. DISTRIBUTION STATEMENT This document has been approved for public release and sale; its distribution is unlimited.		
11. SUPPLEMENTARY NOTES		12. SPONSORING MILITARY ACTIVITY Defense Atomic Support Agency
13. ABSTRACT Computer codes which attempt to solve free-field ground shock problems should be based on mathematically defined constitutive models which realistically simulate the behavior of actual earth materials. Laboratory uniaxial strain and triaxial compression test data are presented to illustrate the effects of various factors such as loading rate, history of unloading-reloading, degree of saturation, weathering, geostatic stress and confining pressure on the stress-strain and strength properties used in soil constitutive relations. The factor which stands out as having by far the most influence on constitutive behavior is the state of stress to which the soil sample (or earth mass) is subjected. An attempt is being made to develop a completely nonlinear-inelastic constitutive model that, when subjected to the particular state of stress used in a laboratory property test, will essentially mirror the test results.		

DD FORM 1473

REPLACES DD FORM 1473, 1 JAN 64, WHICH IS OBSOLETE FOR ARMY USE.

Unclassified

Security Classification

Unclassified

Security Classification

14. KEY WORDS	LINK A		LINK B		LINK C	
	ROLE	WT	ROLE	WT	ROLE	WT
Engineering models						
Ground shock						
Soils -- Dynamic loading						

Unclassified

Security Classification